
Why Ask One When You Can Ask k ? Two-Stage Learning-to-Defer to the Top- k Experts

Yannis Montreuil

School of Computing
National University of Singapore
Singapore, 118431, Singapore
yannis.montreuil@u.nus.edu

Axel Carlier

Institut de Recherche en Informatique de Toulouse
Institut National Polytechnique de Toulouse
Toulouse, 31000, France
axel.carlier@toulouse-inp.fr

Lai Xing Ng

Institute for Infocomm Research
Agency for Science, Technology and Research
Singapore, 138632, Singapore
ng_lai_xing@i2r.a-star.edu.sg

Wei Tsang Ooi

School of Computing
National University of Singapore
Singapore, 118431, Singapore
ooiwt@comp.nus.edu.sg

Abstract

Although existing Learning-to-Defer (L2D) frameworks support multiple experts, they allocate each query to a single expert, limiting their ability to leverage collective expertise in complex decision-making scenarios. To address this, we introduce the *first framework for Top- k Learning-to-Defer*, enabling systems to defer each query to the k most cost-effective experts. Our formulation strictly generalizes classical two-stage L2D by supporting multi-expert deferral—a capability absent in prior work. We further propose *Top- $k(x)$ Learning-to-Defer*, an adaptive extension that learns the optimal number of experts per query based on input complexity, expert quality, and consultation cost. We introduce a novel surrogate loss that is Bayes-consistent, $(\mathcal{R}, \mathcal{G})$ -consistent, and independent of the cardinality parameter k , enabling efficient reuse across different values of k . We show that classical model cascades arise as a special case of our method, situating our framework as a strict generalization of both selective deferral and cascaded inference. Experiments on classification and regression demonstrate that Top- k and Top- $k(x)$ yield improved accuracy–cost trade-offs, establishing a new direction for multi-expert deferral in Learning-to-Defer.

1 Introduction

Learning-to-Defer (L2D) enables models to improve reliability by deferring uncertain predictions to more competent agents (Madras et al., 2018; Mozannar and Sontag, 2020; Verma et al., 2022). By coordinating decisions across a heterogeneous pool of AI models, human experts, or other decision-makers, L2D balances predictive accuracy and consultation cost—two objectives that often trade off in real-world systems. In the *two-stage* variant, all agents are trained offline, and a separate allocation function is learned to route each query to the most cost-effective expert (Narasimhan et al., 2022; Mao et al., 2023a). This setup is particularly useful when retraining the main model is costly or impractical, allowing it to handle routine inputs, while ambiguous or high-risk cases are deferred to larger, more specialized models.

Despite their practical utility, existing Learning-to-Defer frameworks typically assume that each query is allocated to *exactly one agent*. While effective in controlled settings, this single-agent deferral policy falls short in complex, risk-sensitive scenarios where collective expertise is essential. Relying on a

single decision-maker can result in incomplete assessments, heightened susceptibility to individual biases, and increased risk of errors or adversarial manipulation. In contrast, many real-world applications—such as cancer diagnosis, legal deliberation, and fraud detection—require aggregating insights from multiple experts to ensure robust, fair, and accountable outcomes. For instance, in oncology, multidisciplinary tumor boards—comprising radiologists, pathologists, oncologists, and surgeons—collaboratively evaluate patient cases to enhance diagnostic accuracy and mitigate individual error (Jiang et al., 1999; Fatima et al., 2017). Similar multi-agent decision processes arise in cybersecurity, judicial review, and financial risk assessment (Dietterich, 2000), underscoring the need for L2D frameworks that support deferral to multiple agents per query.

Motivated by this limitation, we extend the classical Two-Stage Learning-to-Defer framework to a novel *Top-k* L2D formulation, which allocates each query to the k most reliable agents, ranked by their predictive confidence. To further enhance flexibility and cost-efficiency, we introduce *Top-k(x)* L2D, an adaptive mechanism that learns the optimal number of agents to consult per query, based on input complexity, the distribution of agent competencies, and consultation costs. As a key theoretical insight, we show that classical model cascades (Viola and Jones, 2001; Saberian and Vasconcelos, 2014; Laskaridis et al., 2021; Dohan et al., 2022; Jitkrittum et al., 2023) arise as a restricted special case of both *Top-k* and *Top-k(x)* L2D—corresponding to fixed agent orderings, manually specified thresholds, and early stopping. By leveraging collective expertise, our framework significantly improves predictive performance in collaborative decision-making settings. Our contributions are summarized as follows:

1. **Top-k L2D: Generalized Deferral to Multiple Agents.** We introduce *Top-k Learning-to-Defer*, a novel generalization of the classical Two-Stage L2D framework that allocates each query to a set of the top- k most reliable agents (Section 4.1). This design addresses the limitations of single-agent deferral by supporting collaborative decision-making.
2. **Rigorous Theoretical Guarantees.** We introduce a novel surrogate loss and prove that it is both Bayes-consistent and $(\mathcal{R}, \mathcal{G})$ -consistent for any surrogate derived from the composite-sum loss and any non-negative cost structure. This guarantees convergence toward the Bayes-optimal top- k deferral policy generalizing the top-1 policy from Narasimhan et al. (2022); Mao et al. (2023a) (Section 4.3).
3. **Top-k(x) L2D: Adaptive Agent Selection.** We propose *Top-k(x) Learning-to-Defer*, an adaptive extension that learns the optimal number of agents to consult per query by jointly accounting for input complexity, agent competencies, and consultation costs (Section 4.4).
4. **Model Cascades as a Special Case.** As a key theoretical insight, we show that the classical model cascades paradigm arises as a special case of both *Top-k* and *Top-k(x)* L2D, positioning our framework as a strict generalization of existing approaches. See Section 5 and Appendices A.5 and A.6 for more details.
5. **Extensive Empirical Validation.** We empirically validate our framework on diverse classification and regression benchmarks, where both *Top-k* and *Top-k(x)* L2D consistently outperform competitive baselines (Section 6).

2 Related Work

Two-Stage Learning-to-Defer. The two-stage Learning-to-Defer framework, introduced by Narasimhan et al. (2022); Mao et al. (2023a), comprises a primary model and multiple experts trained offline, whereas in *one-stage* L2D, the main model is trained jointly with the allocation function (Madras et al., 2018; Mozannar and Sontag, 2020; Verma et al., 2022). An independent function, the *rejector*, is subsequently learned to route queries to the most appropriate agent. Recent extensions include regression-focused models (Mao et al., 2024b), multi-task settings (Montreuil et al., 2024), robustness (Montreuil et al., 2025a), and diverse applications (Strong et al., 2024; Palomba et al., 2025; Montreuil et al., 2025b).

Consistency in Top-k Classification. Top- k classification generalizes standard classification by predicting a set of top-ranked classes rather than a single most probable class. Early research introduced top- k hinge loss variants (Lapin et al., 2015, 2016), which were later shown to lack Bayes consistency (Yang and Koyejo, 2020). Alternative non-convex approaches encountered practical optimization challenges (Yang and Koyejo, 2020; Thilagar et al., 2022). Recent advances by Cortes

et al. (2024) have established the Bayes-consistency and \mathcal{H} -consistency of several surrogate losses, including cross-entropy (Mao et al., 2023b) and constrained losses (Cortes and Vapnik, 1995), significantly enhancing the theoretical understanding of top- k classification.

Our Contribution. We bridge the gap between two-stage Learning-to-Defer and top- k classification by introducing a novel framework that enables deferral to multiple experts simultaneously, rather than relying on a single agent. To the best of our knowledge, this intersection has not been previously explored. By unifying these two research directions, our work opens new avenues for more robust and collaborative decision-making. We believe it can have a significant impact in domains where reliability and cost-efficiency are critical.

3 Preliminaries

Let \mathcal{X} be the input space and let \mathcal{Z} denote an arbitrary¹ output space. Each example $(x, z) \in \mathcal{X} \times \mathcal{Z}$ is drawn i.i.d. from an unknown distribution \mathcal{D} . We consider a general hypothesis class $\mathcal{G} = \{g : \mathcal{X} \rightarrow \mathcal{Z}\}$ with predictions defined as $g(x) \in \mathcal{Z}$. When \mathcal{Z} is finite, g may be instantiated via a scoring function $g : \mathcal{X} \times \mathcal{Z} \rightarrow \mathbb{R}$, with predictions given by $g(x) = \arg \max_{z \in \mathcal{Z}} g(x, z)$. Conversely, when \mathcal{Z} is continuous, g may be any measurable function from \mathcal{X} into \mathcal{Z} .

Top-1 Two-Stage Learning-to-Defer. The Learning-to-Defer framework allocates a query $x \in \mathcal{X}$ to the most suitable *agent*, leveraging their respective competencies to enhance predictive performance (Madras et al., 2018; Mozannar and Sontag, 2020; Verma et al., 2022). Agents consist of a main model g and a set of J experts. Formally, the *set of agents* is defined as $a = \{g, m_1, \dots, m_J\}$ and the *set of indexed agents* as $\mathcal{A} = \{0\} \cup [J]$, where agent 0 corresponds to the main model a_0 (or g), and each expert $j \in [J]$ is denoted by a_j (or m_j). The prediction of each agent a_j is given by

$$a_j(x) = \begin{cases} g(x), & j = 0 \quad (\text{main model}), \\ m_j(x), & j > 0 \quad (\text{expert } j), \end{cases}$$

with predictions $a_j(x) \in \mathcal{Z}$. In the two-stage setting, all agents are trained offline. We have full access to the main model g and experts m_j are available on demand (Mao et al., 2023a, 2024b; Montreuil et al., 2024, 2025b,a).

We introduce a rejector function $r \in \mathcal{R}$, defined as $r : \mathcal{X} \rightarrow \mathcal{A}$, which assigns each query x to an agent based on the highest assigned rejection score $r(x) = \arg \max_{j \in \mathcal{A}} r(x, j)$. This rejector is trained by minimizing appropriate losses, formally defined as follows:

Definition 3.1 (Two-Stage L2D Losses). Let $x \in \mathcal{X}$ be an input, $r \in \mathcal{R}$ a rejector, and a the set of agents. The *true deferral loss* ℓ_{def} and its convex, non-negative, upper-bound surrogate deferral losses Φ_{def}^u are defined as

$$\ell_{\text{def}}(r(x), a(x), z) = \sum_{j=0}^J c_j(a_j(x), z) 1_{r(x)=j}, \quad \Phi_{\text{def}}^u(r, a(x), x, z) = \sum_{j=0}^J \tau_j(a(x), z) \Phi_{01}^u(r, x, j),$$

where $c_j(a_j(x), z) \geq 0$ denotes the bounded cost of assigning the query x to agent j (Madras et al., 2018), and $\tau_j(a(x), z) = \sum_{i \neq j} c_i(a_i(x), z)$ aggregates the costs from all other agents. Specifically, assigning the query to an agent j incurs a cost $c_j(a_j(x), z) = \alpha_j \psi(a_j(x), z) + \beta_j$. Here, $\psi : \mathcal{Z} \times \mathcal{Z} \rightarrow \mathbb{R}_+$ quantifies prediction error, β_j represents a consultation cost, and α_j is a scaling factor. In classification, the function ψ corresponds to the standard 0-1 loss, whereas in regression, ψ represents a non-negative regression loss. The special case $\alpha_j = 0$ recovers the learning-with-abstention setting (Chow, 1970; Cortes et al., 2016).

Top- k Classification. Consider a multiclass classification setting, where each input $x \in \mathcal{X}$ is assigned one of $|\mathcal{Y}|$ possible labels $y \in \mathcal{Y}$ (Lapin et al., 2016; Yang and Koyejo, 2020). Let us define a classifier $h : \mathcal{X} \rightarrow \mathcal{Y}$ with hypothesis \mathcal{H} . Given an integer $k \leq |\mathcal{Y}|$, we define the *prediction set* $H_k(x)$ as the set containing the k labels with the highest scores according to $h(x, \cdot)$. Specifically, let

¹Typical choices are $\mathcal{Z} = \mathcal{Y}$ with $\mathcal{Y} = \{1, \dots, n\}$ for multi-class classification, or $\mathcal{Z} = \mathcal{T} \subseteq \mathbb{R}$ for regression, but the theory does not require any special structure on \mathcal{Z} .

the labels be ordered such that $h(x, h_{[1]_h^\downarrow}(x)) \geq h(x, h_{[2]_h^\downarrow}(x)) \geq \dots \geq h(x, h_{[k]_h^\downarrow}(x))$, where the subscript notation $[i]_h^\downarrow$ indicates that the ordering is induced by the descending values of $h(x, \cdot)$. We formally define this permutation notation in Appendix A.1. Accordingly, we introduce

$$H_k(x) = \{h_{[1]_h^\downarrow}(x), h_{[2]_h^\downarrow}(x), \dots, h_{[k]_h^\downarrow}(x)\} = \{[1]_h^\downarrow, [2]_h^\downarrow, \dots, [k]_h^\downarrow\}. \quad (1)$$

When $k = 1$, we recover the standard single-label prediction $h_{[1]_h^\downarrow}(x) = \arg \max_{y \in \mathcal{Y}} h(x, y)$. Conversely, setting $k = |\mathcal{Y}|$ yields the entire label set \mathcal{Y} . To quantify prediction errors, the usual 0-1 loss is extended to the *top-k loss*, defined as $\ell_k(H_k(x), y) = 1_{y \notin H_k(x)}$.

The top- k loss ℓ_k is discontinuous with respect to the scores $\{h(x, y) : y \in \mathcal{Y}\}$, rendering direct optimization computationally infeasible (Lapin et al., 2017, 2016; Yang and Koyejo, 2020; Thilagar et al., 2022; Cortes et al., 2024). Therefore, practical training methods rely on differentiable surrogate losses, which approximate ℓ_k and enable gradient-based optimization (Zhang, 2002; Steinwart, 2007; Bartlett et al., 2006).

Top- k Consistency The main objective is to identify a classifier $h \in \mathcal{H}$ that minimizes the true top- k error $\mathcal{E}_{\ell_k}(h)$, defined as $\mathcal{E}_{\ell_k}(h) = \mathbb{E}_{(x,y)}[\ell_k(H_k(x), y)]$. The Bayes-optimal error is expressed as $\mathcal{E}_{\ell_k}^B(\mathcal{H}) = \inf_{h \in \mathcal{H}} \mathcal{E}_{\ell_k}(h)$. However, minimizing $\mathcal{E}_{\ell_k}(h)$ directly is challenging due to the non-differentiability of the *true multiclass* 0-1 loss (Zhang, 2002; Steinwart, 2007; Awasthi et al., 2022) and by extension, the top- k loss (Lapin et al., 2017, 2016; Yang and Koyejo, 2020; Thilagar et al., 2022; Cortes et al., 2024). To address this challenge, surrogate losses are employed as convex, non-negative upper bounds on ℓ_k . A notable family of multiclass surrogates of the top- k loss is the comp-sum (Lapin et al., 2016; Yang and Koyejo, 2020; Cortes et al., 2024), defined as:

$$\Phi_{01}^u(h, x, y) = \Psi^u \left(\sum_{y' \neq y} \Psi_e(h(x, y) - h(x, y')) \right), \quad (2)$$

where $\Psi_e(v) = \exp(-v)$, which defines the cross-entropy family (Mao et al., 2023b; Wang and Scott, 2023). For $u > 0$, the transformation is given by:

$$\Psi^u(v) = \begin{cases} \log(1 + v) & \text{if } u = 1, \\ \frac{1}{1-u} [(1 - v)^{1-u} - 1] & \text{if } u > 0 \wedge u \neq 1. \end{cases} \quad (3)$$

This formulation generalizes several well-known loss functions, including the sum-exponential loss (Weston and Watkins, 1998), logistic loss (Ohn Aldrich, 1997), generalized cross-entropy (Zhang and Sabuncu, 2018), and mean absolute error loss (Ghosh et al., 2017). The corresponding true error for Φ_{01}^u is defined as $\mathcal{E}_{\Phi_{01}^u}(h) = \mathbb{E}_{(x,y)}[\Phi_{01}^u(h, x, y)]$, with its optimal value expressed as $\mathcal{E}_{\Phi_{01}^u}^*(\mathcal{H}) = \inf_{h \in \mathcal{H}} \mathcal{E}_{\Phi_{01}^u}(h)$. A key property of a surrogate loss is *consistency*, which ensures that minimizing the surrogate excess risk leads to minimizing the true excess risk (Zhang, 2002; Bartlett et al., 2006; Steinwart, 2007; Tewari and Bartlett, 2007). To characterize consistency with a particular hypothesis set \mathcal{H} , Awasthi et al. (2022) introduced \mathcal{H} -consistency bounds.

Theorem 3.2 (\mathcal{H} -consistency bounds). *The surrogate Φ_{01}^u is \mathcal{H} -consistent with respect to ℓ_k if there exists a non-decreasing function $\Gamma^u : \mathbb{R}^+ \rightarrow \mathbb{R}^+$ such that for any distribution \mathcal{D} , the following holds,*

$$\mathcal{E}_{\ell_k}(h) - \mathcal{E}_{\ell_k}^B(\mathcal{H}) + \mathcal{U}_{\ell_k}(\mathcal{H}) \leq \Gamma^u \left(\mathcal{E}_{\Phi_{01}^u}(h) - \mathcal{E}_{\Phi_{01}^u}^*(\mathcal{H}) + \mathcal{U}_{\Phi_{01}^u}(\mathcal{H}) \right),$$

where the minimizability gap $\mathcal{U}_{\ell_{01}}(\mathcal{H})$ quantifies the difference between the best-in-class excess risk and the expected pointwise minimum error: $\mathcal{U}_{\ell_{01}}(\mathcal{H}) = \mathcal{E}_{\ell_k}^B(\mathcal{H}) - \mathbb{E}_x [\inf_{h \in \mathcal{H}} \mathbb{E}_{y|x} [\ell_k(H_k(x), y)]]$. The gap vanishes when $\mathcal{H} = \mathcal{H}_{\text{all}}$ and recovers Bayes-consistency by taking the asymptotic limit (Zhang, 2002; Steinwart, 2007; Bartlett et al., 2006; Awasthi et al., 2022).

4 Top- k Learning-to-Defer: Allocating a Query to the Top- k Agents

Existing Two-Stage Learning-to-Defer frameworks (Mao et al., 2023a, 2024b; Montreuil et al., 2024, 2025a,b) predominantly focus on selecting a single most suitable agent to handle each query x . While theoretically grounded, this one-to-one allocation can be limiting in scenarios characterized by uncertainty, high complexity, or elevated decision risk.

To address these limitations, we propose a novel framework in which each query is allocated to a *set* of the k most cost-effective agents. In what follows, we present our method for learning to allocate each query to the top- k agents based on their deferral scores. A visual comparison between our approach and existing baselines is provided in Appendix A.2.

4.1 Formulating the Top- k Learning-to-Defer Problem

In standard Two-Stage Learning-to-Defer, a rejector $r \in \mathcal{R}$ assigns each query $x \in \mathcal{X}$ to exactly one agent by minimizing the deferral loss ℓ_{def} introduced in Definition 3.1. We generalize the single-agent selection to a top- k agent selection through the *rejector set*.

Definition 4.1 (Rejector Set). Given a query $x \in \mathcal{X}$, a rejector function $r \in \mathcal{R}$ assigns a rejection score $r(x, j)$ to each agent $j \in \mathcal{A}$. For the number of queried agents $k \leq |\mathcal{A}|$, the *rejector set* $R_k(x)$ consists of the indices of the top- k agents ranked by these scores:

$$R_k(x) = \{r_{[0]_r^\downarrow}(x), r_{[1]_r^\downarrow}(x), \dots, r_{[k-1]_r^\downarrow}(x)\} = \{[0]_r^\downarrow, [1]_r^\downarrow, \dots, [k-1]_r^\downarrow\},$$

where the indices satisfy the ordering

$$r(x, r_{[0]_r^\downarrow}(x)) \geq r(x, r_{[1]_r^\downarrow}(x)) \geq \dots \geq r(x, r_{[k-1]_r^\downarrow}(x)).$$

Here, k denotes the number of agents selected to make a prediction and thus the cardinality of the rejector set. The agent with the highest rejection score is given by $r_{[0]_r^\downarrow}(x) = \arg \max_{j \in \mathcal{A}} r(x, j)$, where $r(x, j)$ denotes the score assigned to agent j . More generally, $r_{[k-1]_r^\downarrow}(x)$ refers to the agent ranked k -th in descending order of these scores, according to the ordering induced by $r(x, \cdot)$.

Using the rejector set, we adapt the single-agent deferral loss to define the *top- k deferral loss*, designed explicitly for scenarios involving multiple selected agents:

Lemma 4.2 (Top- k Deferral Loss). *Let $x \in \mathcal{X}$ be a query and $R_k(x) \subseteq \mathcal{A}$ the rejector set from Definition 4.1. The top- k deferral loss is defined as:*

$$\ell_{\text{def},k}(R_k(x), a(x), z) = \sum_{j=0}^J c_j(a_j(x), z) \mathbb{1}_{j \in R_k(x)}.$$

The proof of Lemma 4.2 is provided in Appendix A.7. Intuitively, this loss aggregates the individual costs $c_j(a_j(x), z)$ associated with each agent in the rejector set $R_k(x)$. For instance, consider a scenario with three agents $\mathcal{A} = \{0, 1, 2\}$ and a rejector set $R_2(x) = \{2, 1\}$. Here, the top-2 deferral loss explicitly computes the combined cost $c_2(m_2(x), z) + c_1(m_1(x), z)$, reflecting that both agents 2 and 1 handle the query x , with agent 2 having the highest rejector score.

Remark 1. Assigning $k = 1$ reduces to the single-agent selection scenario, recovering the standard deferral loss introduced in Definition 3.1.

4.2 Top- k L2D: Surrogates for the Top- k Deferral Loss

Similar to the top- k multiclass classification problem, we require a surrogate loss to approximate the novel top- k deferral loss introduced in Lemma 4.4. To construct such surrogates, we rely on the cross-entropy family of surrogate losses Φ_{01}^u defined in Section 3. These surrogates provide convex, non-negative upper bounds for the top- k loss ℓ_k (Lapin et al., 2016; Yang and Koyejo, 2020; Cortes et al., 2024). Leveraging these properties, we first formalize an explicit upper bound on the top- k deferral loss.

Lemma 4.3 (Upper-Bounding the Top- k Deferral Loss). *Let $x \in \mathcal{X}$ be an input, and $k \leq |\mathcal{A}|$ the size of the rejector set. Then, the top- k deferral loss satisfies:*

$$\ell_{\text{def},k}(R_k(x), a(x), z) \leq \sum_{j=0}^J \tau_j(a(x), z) \Phi_{01}^u(r, x, j) - (J - k) \sum_{j=0}^J c_j(a_j(x), z).$$

The detailed proof is provided in Appendix A.8. Choosing $k = 1$ recovers the formulation from prior works established in Mao et al. (2024b); Montreuil et al. (2024, 2025a). This bound explicitly

highlights the relationship between the top- k deferral loss, the cardinality k , and the number of experts J . Crucially, the second term of the upper bound does not depend on the rejector function $r \in \mathcal{R}$. This observation allows us to define a surrogate family independent of the parameter k , as shown in Appendix A.9.

Corollary 4.4 (Surrogates for the Top- k Deferral Loss). *Let $x \in \mathcal{X}$ be an input. The surrogates for the top- k deferral loss are defined as*

$$\Phi_{\text{def},k}^u(r, a(x), x, z) = \sum_{j=0}^J \tau_j(a(x), z) \Phi_{01}^u(r, x, j),$$

whose minimization is notably independent of the cardinality parameter k .

We provide the corresponding training procedure in Algorithm 1 and report the computational complexity for both training and inference in Section A.3. Notably, the proposed surrogate family is independent of the specific choice of rejector set $R_k(x)$ and its cardinality k . As a result, it is unnecessary to train separate rejectors for different values of k , making this surrogate family both computationally efficient and broadly applicable. It is worth noting that these surrogates coincide exactly with the single-expert allocation objective introduced in Definition 3.1.

Although $\Phi_{\text{def},k}^u$ are convex, non-negative surrogates that upper-bound the top- k deferral loss and are independent of k , these properties alone do not guarantee that minimizing them yields a Bayes-optimal rejector set $R_k^B(x)$. To address this, we first formalize the Bayes-optimal rejector set $R_k^B(x)$ in the next subsection. We then provide a rigorous consistency analysis, proving that minimizing $\Phi_{\text{def},k}^u$ is both Bayes-consistent and $(\mathcal{R}, \mathcal{G})$ -consistent.

4.3 Theoretical Guarantees

4.3.1 Optimality of the Rejector Set

We begin by analyzing the optimal selection of agents within the rejector set $R_k(x)$. In the top-1 Two-Stage L2D framework, the Bayes-optimal rejector $r^B(x)$ assigns each query to the agent minimizing the expected cost according to the Bayes-optimal rule $r^B(x) = \arg \min_{j \in \mathcal{A}} \bar{c}_j^*(a_j(x), z)$, where $\bar{c}_0^*(a_0(x), z) = \inf_{g \in \mathcal{G}} \mathbb{E}_{z|x} [c_0(g(x), z)]$ and $\bar{c}_{j>0}^*(a_j(x), z) = \mathbb{E}_{z|x} [c_j(m_j(x), z)]$, as established by Narasimhan et al. (2022); Mao et al. (2023a, 2024b); Montreuil et al. (2024).

In contrast, our proposed Top- k L2D framework generalizes the Bayes-optimal rule by allocating each query to a ranked set of the top- k agents, thereby yielding a more expressive and flexible allocation policy.

Lemma 4.5 (Bayes-optimal Rejector Set). *For a given query $x \in \mathcal{X}$, the Bayes-optimal rejector set $R_k^B(x)$ is defined as the subset of k agents with the lowest expected costs, ordered in increasing cost:*

$$R_k^B(x) = \arg \min_{\substack{R_k(x) \subseteq \mathcal{A} \\ |R_k(x)|=k}} \sum_{j \in R_k(x)} \bar{c}_j^*(a_j(x), z) = \{[0]_{\bar{c}^*}^\dagger, [1]_{\bar{c}^*}^\dagger, \dots, [k-1]_{\bar{c}^*}^\dagger\},$$

where the ordering satisfying $\forall j, j' \in R_k^B(x), j < j' \implies \bar{c}_j^*(a_j(x), z) \leq \bar{c}_{j'}^*(a_{j'}(x), z)$.

The proof of Lemma 4.5 is given in Appendix A.10. This Bayes-optimal selection policy identifies the k most cost-effective agents by minimizing the cumulative expected cost, thereby generalizing earlier formulations by Narasimhan et al. (2022); Mao et al. (2023a, 2024b); Montreuil et al. (2024). In particular, the classical single-agent decision rule is recovered as a special case when $k = 1$, where the selected agent satisfies $[0]_{\bar{c}^*}^\dagger = \arg \min_{j \in \mathcal{A}} \bar{c}_j^*(a_j(x), z)$.

4.3.2 Consistency of Top- k Deferral Surrogates

Establishing the consistency of surrogate losses ensures that minimizing surrogates asymptotically recovers the Bayes-optimal deferral strategy, as shown in Lemma 4.5. While recent work by Cortes et al. (2024) has proven that the cross-entropy family of surrogates Φ_{01}^u is both Bayes-consistent and \mathcal{H} -consistent with respect to the top- k classification loss, the consistency of the top- k deferral surrogates remains an open question and necessitates dedicated theoretical analysis, as done previously

in top-1 classification and regression (Mozannar and Sontag, 2020; Verma et al., 2022; Mao et al., 2024a,b).

To address this gap, we focus on hypothesis classes \mathcal{R} that are *regular for top- k classification*, meaning that the rejector set $R_{|\mathcal{A}|}(x)$ consists of distinct elements covering all agent indices in \mathcal{A} . Additionally, we assume that \mathcal{R} is both *symmetric* and *complete*. Symmetry requires that the hypothesis class \mathcal{R} is invariant under permutations of the agent indices $j \in \mathcal{A}$, reflecting the fact that the ordering of agents is irrelevant in Learning-to-Defer settings. Completeness ensures that the rejector scores $r(x, j)$ can take arbitrary real values, i.e., their range spans \mathbb{R} . These assumptions are mild and satisfied by standard hypothesis classes such as \mathcal{R}_{lin} , \mathcal{R}_{NN} , and \mathcal{R}_{all} .

Under these mild assumptions, we present the following consistency theorem, proven in Appendix A.11:

Theorem 4.6 ($(\mathcal{R}, \mathcal{G})$ -Consistency Bound). *Let $x \in \mathcal{X}$, and consider a hypothesis class \mathcal{R} that is regular, complete, and symmetric, along with any distribution \mathcal{D} . Suppose the cross-entropy surrogate family is \mathcal{R} -consistent. Then, there exists a non-decreasing, non-negative, concave function $\Gamma^u : \mathbb{R}^+ \rightarrow \mathbb{R}^+$, associated with the top- k loss ℓ_k and any surrogate from the cross-entropy family parameterized with u , such that the following bound holds:*

$$\begin{aligned} \mathcal{E}_{\ell_{\text{def},k}}(g, r) - \mathcal{E}_{\ell_{\text{def},k}}^B(\mathcal{G}, \mathcal{R}) - \mathcal{U}_{\ell_{\text{def},k}}(\mathcal{G}, \mathcal{R}) &\leq \tilde{\Gamma}^u \left(\mathcal{E}_{\Phi_{\text{def},k}^u}(r) - \mathcal{E}_{\Phi_{\text{def},k}^u}^*(\mathcal{R}) - \mathcal{U}_{\Phi_{\text{def},k}^u}(\mathcal{R}) \right) \\ &\quad + \mathbb{E}_x \left[\bar{c}_0(g(x), z) - \inf_{g \in \mathcal{G}} \bar{c}_0(g(x), z) \right], \end{aligned}$$

where $\bar{c}_0(g(x), z) = \mathbb{E}_{z|x}[c_0(g(x), z)]$, $Q = \sum_{j=0}^J \mathbb{E}_{z|x}[\tau_j(a(x), z)]$, and $\tilde{\Gamma}^u(v) = Q\Gamma^u\left(\frac{v}{Q}\right)$.

Theorem 4.6 establishes a consistency bound linking the excess risk under the top- k deferral loss $\ell_{\text{def},k}$ to the excess risk under the surrogate family $\Phi_{\text{def},k}^u$. The bound indicates that minimizing the surrogates effectively minimize the original top- k deferral loss, ensuring the optimal rejector set $R_k^*(x)$ approximates the Bayes-optimal rejector set $R_k^B(x)$. If the main model g is near-optimal after offline training, we have $\mathbb{E}_x[\bar{c}_0(g(x), z) - \inf_{g \in \mathcal{G}} \bar{c}_0(g(x), z)] \leq \epsilon$. Furthermore, suppose the surrogate risk satisfies $\mathcal{E}_{\Phi_{\text{def},k}^u}(r) - \mathcal{E}_{\Phi_{\text{def},k}^u}^*(\mathcal{R}) - \mathcal{U}_{\Phi_{\text{def},k}^u}(\mathcal{R}) \leq \epsilon_1$. Then, it follows that

$$\mathcal{E}_{\ell_{\text{def},k}}(g, r) - \mathcal{E}_{\ell_{\text{def},k}}^B(\mathcal{G}, \mathcal{R}) - \mathcal{U}_{\ell_{\text{def},k}}(\mathcal{G}, \mathcal{R}) \leq \tilde{\Gamma}^u(\epsilon_1) + \epsilon, \quad (4)$$

confirming the surrogates' effectiveness in approximating the Bayes-optimal decision rule from Lemma 4.5. Consequently, by considering a learned rejector set $\hat{R}_k(x)$ that minimizes the surrogate risk, we ensure that it reliably approximation the Bayes-optimal policy $R_k^B(x)$.

Remark 2. The minimizability gaps vanish under realizable distributions, or when the hypothesis classes are unrestricted, i.e., $\mathcal{R} = \mathcal{R}_{\text{all}}$ and $\mathcal{G} = \mathcal{G}_{\text{all}}$. Montreuil et al. (2024) formalized a closed-form expression of the minimizability gap, which continues to apply in our current setting. Moreover, when applying these assumptions to Theorem 4.6, the asymptotic excess risk bound reduces to zero, thereby recovering the standard notion of Bayes consistency.

4.4 Top- $k(x)$ L2D: Learning to Select the Optimal Number of Agents Per Query

Motivation. While previous sections established the Bayes and $(\mathcal{R}, \mathcal{G})$ -consistency of our surrogate losses—guaranteeing convergence to the Bayes-optimal rejector set $R_k^B(x)$ —they assume a fixed cardinality k across all queries. *How should one choose the appropriate number of agents k to query at test time?* Choosing a larger k can enhance decision reliability by aggregating diverse expert opinions; however, it also incurs higher consultation costs and increases the risk of including less competent or erroneous agents. Conversely, a smaller value of k reduces computational and monetary costs but may lead to compromised prediction accuracy, particularly in complex or uncertain scenarios.

The Top- k L2D framework enforces a uniform query budget, leading to a fixed expected cardinality $\mathbb{E}_x[|R_k(x)|] = k$. In contrast, we propose learning an instance-dependent query size $k(x)$, tailored to each input. This adaptive strategy reduces the average number of consulted agents, $\mathbb{E}_x[k(x)] \leq k$, without compromising accuracy.

Formulation. To address the adaptive selection of the number of agents, we build upon the framework recently introduced by Cortes et al. (2024). Our objective is to minimize the cardinality of a previously learned full rejector set $\hat{R}_{|\mathcal{A}|}(x)$, while preserving high decision accuracy. To this end, we introduce a *selector function* $s : \mathcal{X} \rightarrow \mathcal{A}$, drawn from a hypothesis class \mathcal{S} . Specifically, the adaptive number of agents is given by $k(x) = s(x) + 1$, where $s(x) = \arg \max_{i \in \mathcal{A}} s(x, i)$. The corresponding top- $k(x)$ agents are then selected from the ordered rejector set $\hat{R}_{k(x)}(x)$.

Definition 4.7 (Cardinality Loss for L2D). Let $x \in \mathcal{X}$, a learned rejector set $\hat{R}_{|\mathcal{A}|}(x)$, a chosen metric $d : \mathcal{X} \rightarrow \mathbb{R}^+$, an increasing non-negative function ξ , and a hyperparameter $\lambda \geq 0$. The cardinality loss tailored to our problem is defined as:

$$\ell_{\text{car}}(\hat{R}_{s(x)+1}(x), s(x), a(x), z) = d(\hat{R}_{s(x)+1}(x), s(x), a(x), z) + \lambda \xi \left(\sum_{i=0}^{s(x)} \beta_{[i]_{\hat{r}}}^{\downarrow} \right),$$

using the normalized loss $\tilde{\ell}_{\text{car}}$ leads to the surrogate defined as:

$$\Phi_{\text{car}}(\hat{R}_{|\mathcal{A}|}(x), s, a(x), x, z) = \sum_{v \in \mathcal{A}} (1 - \tilde{\ell}_{\text{car}}(\hat{R}_{v+1}(x), v, a(x), z)) \Phi_{01}^u(s, x, v),$$

The term $d(\hat{R}_{s(x)+1}(x), s(x), a(x), z)$ quantifies the error incurred by the selected rejector set. Common metrics include the top- k loss, 0-1 loss under majority voting, and weighted majority voting (see Appendix A.13). In parallel, the regularization term $\lambda \xi \left(\sum_{i=0}^{s(x)} \beta_{[i]_{\hat{r}}}^{\downarrow} \right)$ penalizes the unnecessary use of agents that incur consultation costs. Here, ξ is a monotonic function, and $\beta_{[i]_{\hat{r}}}^{\downarrow}$ denotes the cost associated with the agent ranked i -th by the learned rejector \hat{r} . In Appendix A.12, we give the formulation of the Bayes-Optimal selector $s^B(x)$ and show that the rejector set $R_k(x)$ benefits from this optimality.

5 Model Cascades Are Special Cases of Top- k and Top- $k(x)$ L2D

We rigorously show that our Top- k and Top- $k(x)$ L2D frameworks strictly generalize classical model cascades (Viola and Jones, 2001; Saberian and Vasconcelos, 2014; Dohan et al., 2022; Jitkritum et al., 2023), which correspond to a restricted setting with fixed agent orderings, manually specified thresholds, early stopping at the first confident agent, and the absence of consistency guarantees.

In contrast, Top- k L2D is strictly more expressive: it enables input-dependent agent selection, supports querying multiple non-contiguous agents, and adheres to principled consistency properties (see Appendix A.6).

Definition 5.1 (Evaluation order, thresholds, and Size- k cascade allocation). Fix a permutation $\rho = (\rho_0, \rho_1, \dots, \rho_J)$ of \mathcal{A} (the *evaluation order*) and confidence thresholds $0 < \mu_0 < \mu_1 < \dots < \mu_J < 1$. For each agent let $\text{conf} : \mathcal{X} \times \mathcal{A} \rightarrow [0, 1]$ be a confidence function. For a fixed $k \in \{1, \dots, |\mathcal{A}|\}$ define the *cascade set* $\mathcal{K}_k(x) := \{\rho_0, \rho_1, \dots, \rho_{k-1}\}$.

The cascade evaluates the agents in the order ρ until it reaches ρ_{k-1} . If the confidence test $\text{conf}(x, \rho_{k-1}) \geq \mu_{k-1}$ is satisfied, the cascade *allocates* the set $\mathcal{K}_k(x)$; otherwise it proceeds to the next stage (see Section A.5.3 for the adaptive case).

Lemma 5.2 (Score construction). For a fixed k define

$$r_k(x, j) := \begin{cases} 2 - \frac{\text{rank}_{\mathcal{K}_k(x)}(j)}{k+1}, & j \in \mathcal{K}_k(x), \\ -\frac{\text{rank}_{\mathcal{A} \setminus \mathcal{K}_k(x)}(j)}{J+1}, & j \notin \mathcal{K}_k(x), \end{cases}$$

where $\text{rank}_B(j) \in \{1, \dots, |B|\}$ is the index of j inside the list B ordered according to ρ . Then, for every $x \in \mathcal{X}$, the rejector set satisfies $R_k(x) = \mathcal{K}_k(x)$.

This shows that model cascades are special cases of both Top- k and Top- $k(x)$ L2D. We defer proofs as well as the adaptive case in Appendix A.5.

6 Experiments

We evaluate the performance of our proposed methods—*Top-k L2D* and its adaptive extension *Top-k(x) L2D*—against state-of-the-art baselines from the Two-Stage Learning-to-Defer literature (Mao et al., 2023a, 2024b). Our experiments span both classification tasks, including CIFAR-100 (Krizhevsky, 2009) and SVHN (Goodfellow et al., 2013), alongside a regression task on the California Housing dataset (Kelley Pace and Barry, 1997). In all settings, *Top-k* and *Top-k(x) L2D* consistently outperform single-agent deferral baselines across all tasks (Mao et al., 2023a, 2024b).

We report detailed results across multiple evaluation metrics on the California Housing dataset and refer the reader to Appendix A.14 for additional experiments on CIFAR-100 and SVHN, including comparisons with random and oracle *Top-k L2D* baselines. Implementation details and further discussion of the training setup are also provided in Appendix A.14. Evaluation metrics are formally defined in Appendices A.13 and A.14.2. We refer to the *expected budget* $\bar{\beta}(k) = \mathbb{E}_x[\sum_{j=0}^{k-1} \beta_{[j]}]$ and the *expected number of queried agents* $\bar{k} = \mathbb{E}_x[|R_k(x)|]$, where k is fixed for *Top-k L2D* and varies with x in the adaptive *Top-k(x) L2D* setting. Algorithms for both *Top-k* and *Top-k(x) L2D* are provided in Appendix A.1, illustrations in Appendix A.2, and complexities in Appendix A.3.

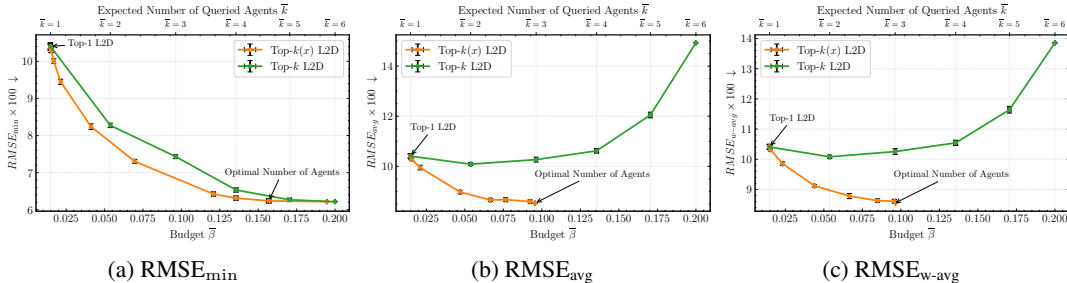


Figure 1: Performance of *Top-k* and *Top-k(x) L2D* across varying budgets $\bar{\beta}$. Each plot reports a different metric: (a) minimum RMSE, (b) uniform average RMSE, and (c) weighted average RMSE (A.14.2). Our approach outperforms the *Top-1 L2D* baseline (Mao et al., 2024b).

In Figure 1a, *Top-k(x)* achieves a near-optimal RMSE of 6.23 with a budget of $\bar{\beta} = 0.156$ and an expected number of agents $\bar{k} = 4.77$, whereas *Top-k* requires the full budget $\bar{\beta} = 0.2$ and $\bar{k} = 6$ agents to reach a comparable score (6.21). This demonstrates the ability of *Top-k(x)* to allocate resources more efficiently by querying only the necessary agents, in contrast to *Top-k*, which tends to over-allocate costly or redundant ones. Additionally, our approach outperforms the *Top-1 L2D* baseline (Mao et al., 2024b), confirming the limitations of single-agent deferral.

Figures 1b and 1c evaluate *Top-k* and *Top-k(x) L2D* under more restrictive metrics— RMSE_{avg} and $\text{RMSE}_{\text{w-avg}}$ —where performance is not necessarily monotonic in the number of queried agents. In these settings, consulting too many or overly expensive agents may degrade overall performance. *Top-k(x)* consistently outperforms *Top-k* by carefully adjusting the number of consulted agents. In both cases, *Top-k(x)* achieves optimal performance using a budget of just $\beta = 0.095$ —a level that *Top-k* fails to attain. For example, in Figure 1b, *Top-k(x)* achieves an $\text{RMSE}_{\text{avg}} = 8.53$, compared to 10.08 for *Top-k*. This demonstrates that our *Top-k(x) L2D* selectively chooses the appropriate agents—when necessary—to enhance the overall system performance.

7 Conclusion

We introduced *Top-k Learning-to-Defer*, a generalization of the two-stage L2D framework that allows deferring queries to multiple agents, and its adaptive extension, *Top-k(x) L2D*, which dynamically selects the number of consulted agents based on input complexity, consultation costs, and the agents’ underlying distributions. We established rigorous theoretical guarantees, including Bayes and $(\mathcal{R}, \mathcal{G})$ -consistency, and showed that model cascades arise as a restricted special case of our framework.

Through experiments on both classification and regression tasks, we demonstrated that *Top-k L2D* consistently outperforms single-agent deferral baselines. Moreover, *Top-k(x) L2D* further improves

performance by achieving comparable or better accuracy at a lower consultation cost. These results highlight the importance of adaptive, cost-aware expert allocation in multi-agent decision systems.

References

- Awasthi, P., Mao, A., Mohri, M., and Zhong, Y. (2022). Multi-class h-consistency bounds. In *Proceedings of the 36th International Conference on Neural Information Processing Systems*, NIPS '22, Red Hook, NY, USA. Curran Associates Inc.
- Bartlett, P., Jordan, M., and McAuliffe, J. (2006). Convexity, classification, and risk bounds. *Journal of the American Statistical Association*, 101:138–156.
- Chow, C. (1970). On optimum recognition error and reject tradeoff. *IEEE Transactions on Information Theory*, 16(1):41–46.
- Cortes, C., DeSalvo, G., and Mohri, M. (2016). Learning with rejection. In Ortner, R., Simon, H. U., and Zilles, S., editors, *Algorithmic Learning Theory*, pages 67–82, Cham. Springer International Publishing.
- Cortes, C., Mao, A., Mohri, C., Mohri, M., and Zhong, Y. (2024). Cardinality-aware set prediction and top- k classification. In *The Thirty-eighth Annual Conference on Neural Information Processing Systems*.
- Cortes, C. and Vapnik, V. N. (1995). Support-vector networks. *Machine Learning*, 20:273–297.
- Dietterich, T. G. (2000). Ensemble methods in machine learning. In *Multiple Classifier Systems*, pages 1–15, Berlin, Heidelberg. Springer Berlin Heidelberg.
- Dohan, D., Xu, W., Lewkowycz, A., Austin, J., Bieber, D., Lopes, R. G., Wu, Y., Michalewski, H., Saurous, R. A., Sohl-Dickstein, J., et al. (2022). Language model cascades. *arXiv preprint arXiv:2207.10342*.
- Fatima, M., Pasha, M., et al. (2017). Survey of machine learning algorithms for disease diagnostic. *Journal of Intelligent Learning Systems and Applications*, 9(01):1.
- Ghosh, A., Kumar, H., and Sastry, P. S. (2017). Robust loss functions under label noise for deep neural networks. In *Proceedings of the Thirty-First AAAI Conference on Artificial Intelligence*, AAAI'17, page 1919–1925. AAAI Press.
- Goodfellow, I. J., Bulatov, Y., Ibarz, J., Arnoud, S., and Shet, V. (2013). Multi-digit number recognition from street view imagery using deep convolutional neural networks. *arXiv preprint arXiv:1312.6082*.
- He, K., Zhang, X., Ren, S., and Sun, J. (2016). Deep residual learning for image recognition. In *Proceedings of the IEEE conference on computer vision and pattern recognition*, pages 770–778.
- Jiang, Y., Nishikawa, R. M., Schmidt, R. A., Metz, C. E., Giger, M. L., and Doi, K. (1999). Improving breast cancer diagnosis with computer-aided diagnosis. *Academic radiology*, 6(1):22–33.
- Jitkrittum, W., Gupta, N., Menon, A. K., Narasimhan, H., Rawat, A., and Kumar, S. (2023). When does confidence-based cascade deferral suffice? *Advances in Neural Information Processing Systems*, 36:9891–9906.
- Kelley Pace, R. and Barry, R. (1997). Sparse spatial autoregressions. *Statistics and Probability Letters*, 33(3):291–297.
- Kingma, D. P. and Ba, J. (2014). Adam: A method for stochastic optimization. *arXiv preprint arXiv:1412.6980*.
- Krizhevsky, A. (2009). Learning multiple layers of features from tiny images.
- Lapin, M., Hein, M., and Schiele, B. (2015). Top-k multiclass svm. *Advances in neural information processing systems*, 28.

- Lapin, M., Hein, M., and Schiele, B. (2016). Loss functions for top-k error: Analysis and insights. In *Proceedings of the IEEE conference on computer vision and pattern recognition*, pages 1468–1477.
- Lapin, M., Hein, M., and Schiele, B. (2017). Analysis and optimization of loss functions for multiclass, top-k, and multilabel classification. *IEEE transactions on pattern analysis and machine intelligence*, 40(7):1533–1554.
- Laskaridis, S., Kouris, A., and Lane, N. D. (2021). Adaptive inference through early-exit networks: Design, challenges and directions. In *Proceedings of the 5th International Workshop on Embedded and Mobile Deep Learning, EMDL’21*, page 1–6, New York, NY, USA. Association for Computing Machinery.
- Loshchilov, I. and Hutter, F. (2017). Decoupled weight decay regularization. *arXiv preprint arXiv:1711.05101*.
- Madras, D., Pitassi, T., and Zemel, R. (2018). Predict responsibly: improving fairness and accuracy by learning to defer. *Advances in neural information processing systems*, 31.
- Mao, A., Mohri, C., Mohri, M., and Zhong, Y. (2023a). Two-stage learning to defer with multiple experts. In *Thirty-seventh Conference on Neural Information Processing Systems*.
- Mao, A., Mohri, M., and Zhong, Y. (2023b). Cross-entropy loss functions: Theoretical analysis and applications. In *International conference on Machine learning*, pages 23803–23828. PMLR.
- Mao, A., Mohri, M., and Zhong, Y. (2024a). Principled approaches for learning to defer with multiple experts.
- Mao, A., Mohri, M., and Zhong, Y. (2024b). Regression with multi-expert deferral. In *Proceedings of the 41st International Conference on Machine Learning, ICML’24*. JMLR.org.
- Montreuil, Y., Carlier, A., Ng, L. X., and Ooi, W. T. (2025a). Adversarial robustness in two-stage learning-to-defer: Algorithms and guarantees.
- Montreuil, Y., Yeo, S. H., Carlier, A., Ng, L. X., and Ooi, W. T. (2024). Two-stage learning-to-defer for multi-task learning. *arXiv preprint arXiv:2410.15729*.
- Montreuil, Y., Yeo, S. H., Carlier, A., Ng, L. X., and Ooi, W. T. (2025b). Optimal query allocation in extractive qa with llms: A learning-to-defer framework with theoretical guarantees. *arXiv preprint arXiv:2410.15761*.
- Mozannar, H. and Sontag, D. (2020). Consistent estimators for learning to defer to an expert. In *Proceedings of the 37th International Conference on Machine Learning, ICML’20*. JMLR.org.
- Narasimhan, H., Jitkrittum, W., Menon, A. K., Rawat, A., and Kumar, S. (2022). Post-hoc estimators for learning to defer to an expert. In Koyejo, S., Mohamed, S., Agarwal, A., Belgrave, D., Cho, K., and Oh, A., editors, *Advances in Neural Information Processing Systems*, volume 35, pages 29292–29304. Curran Associates, Inc.
- Ohn Aldrich, R. A. (1997). Fisher and the making of maximum likelihood 1912-1922. *Statistical Science*, 12(3):162–179.
- Palomba, F., Pugnana, A., Alvarez, J. M., and Ruggieri, S. (2025). A causal framework for evaluating deferring systems. In *The 28th International Conference on Artificial Intelligence and Statistics*.
- Radford, A., Kim, J. W., Hallacy, C., Ramesh, A., Goh, G., Agarwal, S., Sastry, G., Askell, A., Mishkin, P., Clark, J., Krueger, G., and Sutskever, I. (2021). Learning transferable visual models from natural language supervision.
- Saberian, M. and Vasconcelos, N. (2014). Boosting algorithms for detector cascade learning. *Journal of Machine Learning Research*, 15(74):2569–2605.
- Steinwart, I. (2007). How to compare different loss functions and their risks. *Constructive Approximation*, 26:225–287.

- Strong, J., Men, Q., and Noble, A. (2024). Towards human-AI collaboration in healthcare: Guided deferral systems with large language models. In *ICML 2024 Workshop on LLMs and Cognition*.
- Tewari, A. and Bartlett, P. L. (2007). On the consistency of multiclass classification methods. *Journal of Machine Learning Research*, 8(36):1007–1025.
- Thilagar, A., Frongillo, R., Finocchiaro, J. J., and Goodwill, E. (2022). Consistent polyhedral surrogates for top-k classification and variants. In Chaudhuri, K., Jegelka, S., Song, L., Szepesvari, C., Niu, G., and Sabato, S., editors, *Proceedings of the 39th International Conference on Machine Learning*, volume 162 of *Proceedings of Machine Learning Research*, pages 21329–21359. PMLR.
- Verma, R., Barrejon, D., and Nalisnick, E. (2022). Learning to defer to multiple experts: Consistent surrogate losses, confidence calibration, and conformal ensembles. In *International Conference on Artificial Intelligence and Statistics*.
- Viola, P. and Jones, M. (2001). Rapid object detection using a boosted cascade of simple features. In *Proceedings of the 2001 IEEE Computer Society Conference on Computer Vision and Pattern Recognition. CVPR 2001*, volume 1, pages I–I.
- Wang, Y. and Scott, C. (2023). On classification-calibration of gamma-phi losses. In Neu, G. and Rosasco, L., editors, *Proceedings of Thirty Sixth Conference on Learning Theory*, volume 195 of *Proceedings of Machine Learning Research*, pages 4929–4951. PMLR.
- Weston, J. and Watkins, C. (1998). Multi-class support vector machines. Technical report, Citeseer.
- Yang, F. and Koyejo, S. (2020). On the consistency of top-k surrogate losses. In *International Conference on Machine Learning*, pages 10727–10735. PMLR.
- Zhang, T. (2002). Statistical behavior and consistency of classification methods based on convex risk minimization. *Annals of Statistics*, 32.
- Zhang, Z. and Sabuncu, M. (2018). Generalized cross entropy loss for training deep neural networks with noisy labels. *Advances in neural information processing systems*, 31.

Contents

1	Introduction	1
2	Related Work	2
3	Preliminaries	3
4	Top-k Learning-to-Defer: Allocating a Query to the Top-k Agents	4
4.1	Formulating the Top- k Learning-to-Defer Problem	5
4.2	Top- k L2D: Surrogates for the Top- k Deferral Loss	5
4.3	Theoretical Guarantees	6
4.3.1	Optimality of the Rejector Set	6
4.3.2	Consistency of Top- k Deferral Surrogates	6
4.4	Top- $k(x)$ L2D: Learning to Select the Optimal Number of Agents Per Query	7
5	Model Cascades Are Special Cases of Top-k and Top-$k(x)$ L2D	8
6	Experiments	9
7	Conclusion	9
A	Appendix	15
A.1	Algorithm	15
A.2	Illustration of Top- $k(x)$ and Top- k L2D	15
A.3	Computational complexity of Top-1, Top- k , and Top- $k(x)$ L2D	17
A.4	Notations for Ordered Sets	17
A.5	Model Cascades Are Special Cases of Top- k and Top- $k(x)$ L2D	18
A.5.1	Model cascades	18
A.5.2	Embedding a fixed- k cascade	19
A.5.3	Embedding adaptive (early-exit) cascades	19
A.6	Expressiveness: Model Cascades vs. Top- k / Top- $k(x)$ L2D	19
A.7	Proof Lemma 4.2	20
A.8	Proof Lemma 4.3	21
A.9	Proof Corollary 4.4	22
A.10	Proof Lemma 4.5	22
A.11	Proof Theorem 4.6	24
A.12	Proof Bayes-Optimal Cardinality Lemma A.8	26
A.13	Choice of the metric d	27
A.14	Experiments	28
A.14.1	Datasets	28
A.14.2	Metrics	28
A.14.3	General Settings for Top- k and Top- $k(x)$ L2D	29

A.14.4 Reproducibility	29
A.14.5 Resources	29
A.14.6 Results on California Housing.	29
A.14.7 Results on SVHN	31
A.14.8 Results on CIFAR100.	32
A.15 Limitations	34

A Appendix

A.1 Algorithm

Algorithm 1 Top- k L2D Training Algorithm

Input: Dataset $\{(x_i, z_i)\}_{i=1}^I$, main model $g \in \mathcal{G}$, experts $m = (m_1, \dots, m_J)$, rejector $r \in \mathcal{R}$, number of epochs EPOCH, batch size BATCH, learning rate μ .

Initialization: Initialize rejector parameters θ .

for $i = 1$ to EPOCH **do**

Shuffle dataset $\{(x_i, z_i)\}_{i=1}^I$.

for each mini-batch $\mathcal{B} \subset \{(x_i, z_i)\}_{i=1}^I$ of size BATCH **do**

Extract input-output pairs $(x, z) \in \mathcal{B}$.

Query model $g(x)$ and experts $m(x)$. { Agents have been trained offline and fixed }

Evaluate aggregated costs $\tau_j(a(x), z)$ for $j \in \mathcal{A}$ agents. { Compute costs }

Compute the empirical risk minimization:

$$\hat{\mathcal{E}}_{\text{def},k}^u(r; \theta) = \frac{1}{\text{BATCH}} \sum_{(x,z) \in \mathcal{B}} \left[\Phi_{\text{def},k}^u(r, a(x), x, z) \right].$$

Update parameters θ :

$$\theta \leftarrow \theta - \mu \nabla_{\theta} \hat{\mathcal{E}}_{\text{def},k}^u(r; \theta). \quad \text{{ Gradient update }}$$

end for

end for

Return: trained rejector model \hat{r} .

Algorithm 2 Cardinality Training Algorithm

Input: Dataset $\{(x_i, z_i)\}_{i=1}^I$, main model $g \in \mathcal{G}$, experts $m = (m_1, \dots, m_J)$, trained rejector \hat{r} from Algorithm 1, selector $s \in \mathcal{S}$, number of epochs EPOCH, batch size BATCH, learning rate μ .

Initialization: Initialize selector parameters θ .

for $i = 1$ to EPOCH **do**

Shuffle dataset $\{(x_i, z_i)\}_{i=1}^I$.

for each mini-batch $\mathcal{B} \subset \{(x_i, z_i)\}_{i=1}^I$ of size BATCH **do**

Extract input-output pairs $(x, z) \in \mathcal{B}$.

Query model $g(x)$ and experts $m(x)$. { Agents have been trained offline and fixed }

Compute the scores $\{\hat{r}(x, j)\}_{j=0}^J$ using the trained rejector \hat{r} .

Sort these scores and select entries to construct the rejector set $\hat{R}_{|\mathcal{A}|}(x)$.

Compute the empirical risk minimization:

$$\hat{\mathcal{E}}_{\text{car}}(s; \theta) = \frac{1}{\text{BATCH}} \sum_{(x,z) \in \mathcal{B}} \left[\Phi_{\text{car}}(\hat{R}_{|\mathcal{A}|}, s, a(x), z) \right].$$

Update parameters θ :

$$\theta \leftarrow \theta - \mu \nabla_{\theta} \hat{\mathcal{E}}_{\text{car}}(s; \theta). \quad \text{{ Gradient update }}$$

end for

end for

Return: trained selector model \hat{s} .

A.2 Illustration of Top- $k(x)$ and Top- k L2D

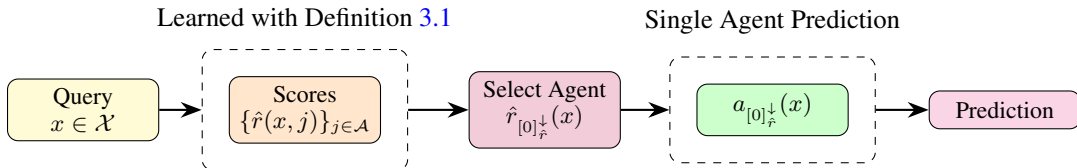


Figure 2: Inference step of Top-1 L2D (Narasimhan et al., 2022; Mao et al., 2023a, 2024b; Montreuil et al., 2024): Given a query, we process it through the rejector. We select the agent with the highest score $r(x) = \arg \max_{j \in \mathcal{A}} r(x, j)$. Then, we query this agent and make the final prediction.

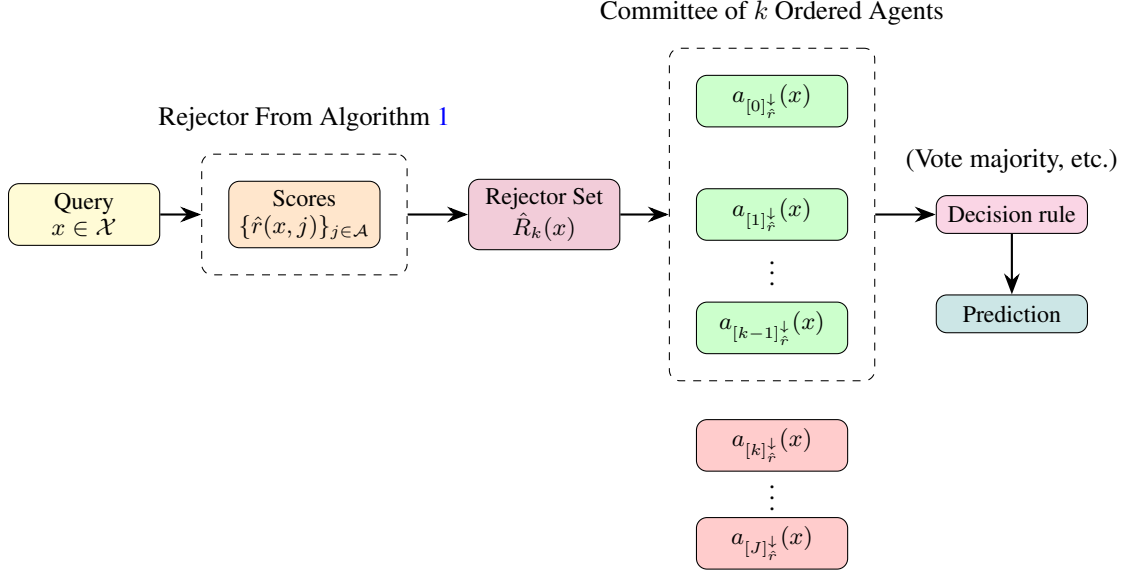


Figure 3: Inference Step of Top- k L2D: Given a query x , we first process it through the rejctor trained using Algorithm 1. Based on this, we select a fixed number k of agents to query, forming the *rejctor set* $R_k(x)$, as defined in Definition 4.1. By construction, the expected size satisfies $\mathbb{E}_x[|R_k(x)|] = k$. We then aggregate predictions from the selected top- k agents using a decision rule—such as majority vote or weighted voting. The final prediction is produced by this committee according to the chosen rule.

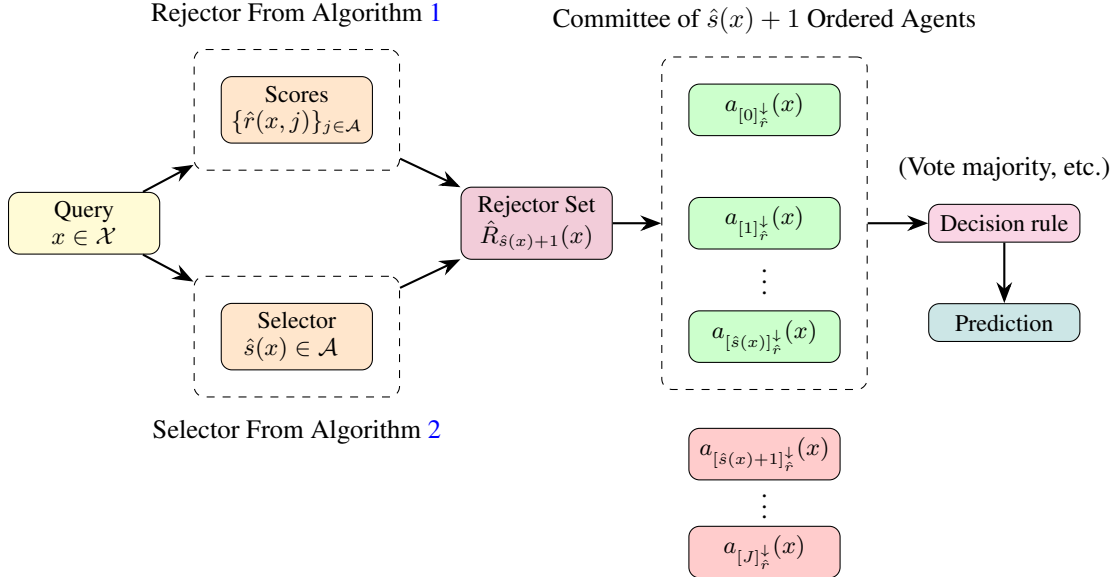


Figure 4: Inference Step of Top- $k(x)$ L2D: Given a query x , we process it through both the rejctor, trained using Algorithm 1, and the selector, trained using Algorithm 2. Based on these two functions, we construct the *rejctor set*, as defined in Definition 4.1. By construction, its expected size satisfies $\mathbb{E}_x[|\hat{R}_{\hat{s}(x)+1}(x)|] = \mathbb{E}_x[k(x)]$. We then aggregate predictions from the top- $(\hat{s}(x) + 1)$ agents using a decision rule (e.g., majority vote, weighted voting). The final prediction is produced by this committee of experts according to the chosen decision rule.

A.3 Computational complexity of Top-1, Top- k , and Top- $k(x)$ L2D

Let $\mathcal{A} = \{0\} \cup [J]$ be the index set of the main model ($j = 0$) and J experts. For a *single* forward-backward pass of the comp-sum surrogate Φ_{01}^u , denote its cost by

$$T_\Phi \quad (\text{time}), \quad M_\Phi \quad (\text{memory}).$$

At inference time let T_r, M_r be the cost of evaluating one rejector score $r(x, j)$. Only Top- $k(x)$ uses a selector $s \in \mathcal{S}$, whose per-score costs are T_s, M_s . In the cardinality surrogate (Def. 4.7) the task-specific metric $d(\cdot)$ contributes T_d time and no additional memory beyond M_Φ .

Training phase.

- **Top-1 and Top- k (fixed k).** Both variants minimise the same deferral surrogate $\Phi_{\text{def}}^u(r, a(x), x, z) = \sum_{j=0}^J \tau_j(a(x), z) \Phi_{01}^u(r, x, j)$, which entails $J + 1$ calls to Φ_{01}^u per example:

$$T_{\text{train}}^{\text{Top-1}/k} = (J + 1)T_\Phi, \quad M_{\text{train}}^{\text{Top-1}/k} = (J + 1)M_\Phi.$$

The fixed value of k plays no rôle during optimisation, so the two costs are identical.

- **Top- $k(x)$ (selector).** The selector is learned with a second surrogate $\Phi_{\text{car}} = \sum_{v=0}^J (1 - \tilde{\ell}_{\text{car}}(\hat{R}_{v+1}(x), v, a(x), z)) \Phi_{01}^u(s, x, v)$, adding another $J + 1$ surrogate calls plus the metric term:

$$T_{\text{train}}^{\text{card}} = (J + 1)(T_\Phi + T_d), \quad M_{\text{train}}^{\text{card}} = (J + 1)M_\Phi.$$

Hence $T_{\text{train}}^{\text{Top-}k(x)} \leq 2(J + 1)T_\Phi + (J + 1)T_d$ and $M_{\text{train}}^{\text{Top-}k(x)} = 2(J + 1)M_\Phi$, i.e., a constant-factor overhead while preserving linear growth in J .

Inference phase. Every variant first computes the score vector $\{r(x, j)\}_{j=0}^J$, which costs

$$T_{\text{scores}} = (J + 1)T_r, \quad M_{\text{scores}} = (J + 1)M_r.$$

The subsequent allocation differs as follows (per input x)²:

Variant	extra time after scores	extra memory
Top-1	$\Theta_{\text{Top-1}} = \Theta(J)$	$\Theta(1)$
Top- k	$\Theta_{\text{Top-}k} \in \{\Theta(J + k \log k), \Theta(J \log J)\}$	$\Theta(k)$
Top- $k(x)$	$\Theta_{\text{Top-}k(x)} = \Theta_{\text{Top-}k} + (J + 1)T_s + \Theta(k(x))$	$\Theta(J) + (J + 1)M_s + \Theta(k(x))$

Explanation. Top- $k(x)$ must (i) fully sort the $J+1$ rejector scores to obtain the ordered list $\hat{R}_{|\mathcal{A}|}(x)$ ($\Theta(J \log J)$ time, $\Theta(J)$ memory), (ii) compute the selector scores $\{s(x, v)\}_{v=0}^J$ ($(J+1)T_s$ time, $(J+1)M_s$ memory), and (iii) output the first $k(x) = s(x) + 1$ indices ($\Theta(k(x))$ time and memory).

Take-away.

- *Training.* Top-1 and Top- k are identical.
- *Inference.* All methods are dominated by the $(J + 1)$ rejector evaluations ($\mathcal{O}(J)$). Allocation costs are $\Theta(J)$ for Top-1, $\Theta(J + k \log k)$ (or $\Theta(J \log J)$ if a full sort is used) for Top- k , and $\Theta(J \log J) + (J + 1)T_s$ for Top- $k(x)$. Hence the adaptive variant carries the largest overhead but still scales no worse than $\mathcal{O}(J \log J)$ overall.

A.4 Notations for Ordered Sets

Definition A.1 (Orderings on a finite set). Let $\Omega = \{1, \dots, N\}$ be a set of cardinality $N := |\Omega|$ and let

$$f : \mathcal{M} \times \Omega \longrightarrow \mathbb{R}, \quad (m, \omega) \mapsto f(m, \omega),$$

where \mathcal{M} is a measurable input space (typically $\mathcal{M} = \mathcal{X}$ or $\mathcal{M} = \mathcal{X} \times \mathcal{Y}$).

²If k is a small constant (e.g. $k \leq 10$) the heap bound $\Theta(J + k \log k)$ simplifies to $\Theta(J)$. For $k = \Theta(J)$ a linear-time selection algorithm matches the $\Theta(J)$ order.

Descending permutation. For every fixed $m \in \mathcal{M}$, let

$$\pi_f^\downarrow(m) : \Omega \longrightarrow \Omega$$

be the (tie-broken) permutation that satisfies

$$f(m, \pi_f^\downarrow(m)(1)) \geq f(m, \pi_f^\downarrow(m)(2)) \geq \dots \geq f(m, \pi_f^\downarrow(m)(N)).$$

The element occupying the i -th *largest* position is denoted by

$$[i]_f^\downarrow := \pi_f^\downarrow(m)(i), \quad i = 1, \dots, N.$$

Ascending permutation. Analogously, define

$$\pi_f^\uparrow(m) : \Omega \longrightarrow \Omega$$

such that

$$f(m, \pi_f^\uparrow(m)(1)) \leq f(m, \pi_f^\uparrow(m)(2)) \leq \dots \leq f(m, \pi_f^\uparrow(m)(N)),$$

and set

$$[i]_f^\uparrow := \pi_f^\uparrow(m)(i), \quad i = 1, \dots, N.$$

Top- k subset. For $k \in \{0, \dots, J\}$ and an order indicator $o \in \{\downarrow, \uparrow\}$, the *top- k subset* is

$$R_k(x) := \{[0]_f^o, [1]_f^o, \dots, [k-1]_f^o\}.$$

Remark 3 (Typical instantiations). In particular:

1. **Rejector scores.** Take $\Omega = \mathcal{A} = \{0, \dots, J\}$, $\mathcal{M} = \mathcal{X}$, and $f_r(x, j) := r(x, j)$. Descending order ($o = \downarrow$) ranks agents from most to least confident at retaining the query.
2. **Agent-specific consultation costs.** Fix $\Omega = \mathcal{A}$ but enlarge the input space to $\mathcal{M} = \mathcal{X} \times \mathcal{Z}$ and define

$$f_c((x, z), j) := c_j(a_j(x), z).$$
 Ascending order ($o = \uparrow$) lists agents from cheapest to most expensive for the specific pair (x, z) .
3. **Label-wise scores.** Let $\Omega = \mathcal{Y}$ (label set), $\mathcal{M} = \mathcal{X}$, and $f_h(x, y) := h(x, y)$. Either order can be used, depending on whether larger or smaller h -values are preferable for prediction.

A.5 Model Cascades Are Special Cases of Top- k and Top- $k(x)$ L2D

Throughout, let $\mathcal{A} = \{0\} \cup [J]$ be the index set of agents, already introduced in Section 3. For $j \in \mathcal{A}$ we denote by $a_j : \mathcal{X} \rightarrow \mathcal{Z}$ the prediction of agent j , by $r : \mathcal{X} \times \mathcal{A} \rightarrow \mathbb{R}$ a *rejector score*, and by $R_k(x) = \{r_{[0]_f^\downarrow}(x), \dots, r_{[k-1]_f^\downarrow}(x)\}$ the *rejector set* containing the indices of the k largest scores (Definition 4.1).

A.5.1 Model cascades

Definition A.2 (Evaluation order and thresholds). Fix a permutation $\rho = (\rho_0, \rho_1, \dots, \rho_J)$ of \mathcal{A} (the *evaluation order*) and confidence thresholds $0 < \mu_0 < \mu_1 < \dots < \mu_J < 1$. For each agent let $\text{conf} : \mathcal{X} \times \mathcal{A} \rightarrow [0, 1]$ be a confidence measure.

Definition A.3 (Size- k cascade allocation). For a fixed $k \in \{1, \dots, |\mathcal{A}|\}$ define the *cascade set*

$$\mathcal{K}_k(x) := \{\rho_0, \rho_1, \dots, \rho_{k-1}\}.$$

The cascade evaluates the agents in the order ρ until it reaches ρ_{k-1} . If the confidence test $\text{conf}(\rho_{k-1}, x) \geq \mu_{k-1}$ is satisfied, the cascade *allocates* the set $\mathcal{K}_k(x)$; otherwise it proceeds to the next stage (see Section A.5.3 for the adaptive case).

A.5.2 Embedding a fixed- k cascade

Lemma A.4 (Score construction). *For a fixed k define*

$$r_k(x, j) := \begin{cases} 2 - \frac{\text{rank}_{\mathcal{K}_k(x)}(j)}{k+1}, & j \in \mathcal{K}_k(x), \\ -\frac{\text{rank}_{\mathcal{A} \setminus \mathcal{K}_k(x)}(j)}{J+1}, & j \notin \mathcal{K}_k(x), \end{cases}$$

where $\text{rank}_B(j) \in \{1, \dots, |B|\}$ is the index of j inside the list B ordered according to ρ . Then for every $x \in \mathcal{X}$

$$R_k(x) = \mathcal{K}_k(x).$$

Proof. Separation. Scores assigned to $\mathcal{K}_k(x)$ lie in $(1, 2]$, while scores assigned to $\mathcal{A} \setminus \mathcal{K}_k(x)$ lie in $[-1, -\frac{1}{J+1}]$; hence all k largest scores belong exactly to $\mathcal{K}_k(x)$.

Distinctness. Within each block, consecutive ranks differ by $1/(k+1)$ or $1/(J+1)$, so ties cannot occur. Therefore the permutation returns precisely the indices of $\mathcal{K}_k(x)$ in decreasing order, and the rejector set equals $\mathcal{K}_k(x)$. \square

Corollary A.5 (Cascade embedding for any fixed k). *For every $k \in \{1, \dots, |\mathcal{A}|\}$ the rejector r_k of Lemma A.4 satisfies*

$$R_k(x) = \mathcal{K}_k(x) \quad \forall x \in \mathcal{X}.$$

Consequently, the Top- k Learning-to-Defer allocation coincides exactly with the size- k cascade allocation.

Proof. Immediate from Lemma A.4. \square

A.5.3 Embedding adaptive (early-exit) cascades

Let the cascade stop after a *data-dependent* number of stages $k(x) \in \{1, \dots, |\mathcal{A}|\}$. Define the selector $s(x) = k(x) + 1$ (as required in Section 4.4) and reuse the score construction of Lemma A.4 with k replaced by $k(x)$: $r_{k(x)}(x, \cdot)$.

Lemma A.6 (Cascade embedding for adaptive cardinality). *With rejector $r_{k(x)}$ and selector $s(x) = k(x) + 1$ the Top- $k(x)$ Learning-to-Defer pipeline allocates $\mathcal{K}_{k(x)}(x)$ for every input x . Therefore any adaptive (early-exit) model cascade is a special case of Top- $k(x)$ Learning-to-Defer.*

Proof. Applying Lemma A.4 with $k = k(x)$ yields $R_{k(x)}(x) = \mathcal{K}_{k(x)}(x)$. The selector truncates the full rejector set to its first $s(x) + 1 = k(x)$ elements—precisely $\mathcal{K}_{k(x)}(x)$. \square

A.6 Expressiveness: Model Cascades vs. Top- k / Top- $k(x)$ L2D

Hierarchy. Every model cascade can be realised by a suitable choice of rejector scores and, for the adaptive case, a selector (see App. A.5). Hence

$$\underbrace{\text{Model Cascades}}_{\text{prefix of a fixed order}} \subset \underbrace{\text{Top-}k \text{ L2D}}_{\text{constant } k} \subset \underbrace{\text{Top-}k(x) \text{ L2D}}_{\text{learned } k(x)}.$$

The inclusion is *strict*, for the reasons detailed below.

Why the inclusion is strict.

1. **Non-contiguous selection.** A Top- k rejector may pick any subset of size k (e.g. $\{0, 2, 5\}$), whereas a cascade always selects a *prefix* $\{\rho_0, \dots, \rho_{k-1}\}$ of the evaluation order.
2. **Learned cardinality.** In Top- $k(x)$ L2D the selector $s(x)$ is trained by minimising the cardinality surrogate; Theorem 4.6 provides $(\mathcal{R}, \mathcal{G})$ -consistency. Classical cascades rely on fixed confidence thresholds with no statistical guarantee.

3. **Cost-aware ordering.** Lemma 4.5 shows the Bayes-optimal rejector orders agents by *expected cost*, which may vary with x . Cascades usually impose a single, input-independent order ρ .
4. **Multi-expert aggregation.** After selecting k agents, Top- k L2D can aggregate their predictions (majority vote, weighted vote, averaging, *etc.*). A cascade stops at the *first* confident agent and discards all later opinions.

Separating example. Consider three models a_0, a_1, a_2 . A Top-2 policy that always chooses the two most confident models (e.g. $\{0, 2\}$ on some inputs, $\{1, 2\}$ on others) and combines them by weighted voting *cannot* be written as a cascade: no prefix of a fixed order can realise the non-contiguous set $\{0, 2\}$, and cascades output a single agent rather than a pair. Therefore Top- k /Top- $k(x)$ Learning-to-Defer is strictly more expressive than classical model cascades.

A.7 Proof Lemma 4.2

Lemma 4.2 (Top- k Deferral Loss). *Let $x \in \mathcal{X}$ be a query and $R_k(x) \subseteq \mathcal{A}$ the rejector set from Definition 4.1. The top- k deferral loss is defined as:*

$$\ell_{\text{def},k}(R_k(x), a(x), z) = \sum_{j=0}^J c_j(a_j(x), z) \mathbb{1}_{j \in R_k(x)}.$$

Proof. In the standard L2D setting (see 3.1), the deferral loss utilizes the indicator function $\mathbb{1}_{r(x)=j}$ to select the most cost-efficient agent in the system. We can upper-bound the standard L2D loss by employing the indicator function over the rejector set $R_k(x)$:

$$\begin{aligned} \ell_{\text{def}}(r(x), a(x), z) &= \sum_{j=0}^J c_j(a_j(x), z) \mathbb{1}_{r(x)=j} \\ &\leq \sum_{j=0}^J c_j(a_j(x), z) \mathbb{1}_{j \in R_k(x)} \\ &= \ell_{\text{def},k}(R_k(x), a(x), z). \end{aligned} \tag{5}$$

Consider a system with three agents, $\mathcal{A} = \{0, 1, 2\}$, and a rejector set $R_{k=|\mathcal{A}|}(x) = \{2, 1, 0\}$. This indicates that agent 2 has a higher confidence score than agent 1 and 0, i.e., $r(x, 2) \geq r(x, 1) \geq r(x, 0)$. We evaluate $\ell_{\text{def},k}$ for different values of $k \leq |\mathcal{A}|$:

For $k = 1$: The rejector set is $R_1(x) = \{2\}$, which corresponds to the standard L2D setting where deferral is made to the most confident agent (Narasimhan et al., 2022; Mao et al., 2023a). Thus,

$$\ell_{\text{def},1}(R_1(x), a(x), z) = c_2(a_2(x), z), \tag{6}$$

recovering the same result as ℓ_{def} .

For $k = 2$: The rejector set expands to $R_2(x) = \{2, 1\}$, implying that both agent 2 and agent 1 are queried. Therefore,

$$\ell_{\text{def},2}(R_2(x), a(x), z) = c_2(a_2(x), z) + c_1(a_1(x), z), \tag{7}$$

correctly reflecting the computation of costs from the queried agents.

For $k = 3$: The rejector set further extends to $R_3(x) = \{2, 1, 0\}$, implying that all agents in the system are queried. Consequently,

$$\ell_{\text{def},3}(R_3(x), a(x), z) = c_2(a_2(x), z) + c_1(a_1(x), z) + c_0(a_0(x), z), \tag{8}$$

incorporating the costs from all agents in the system. \square

A.8 Proof Lemma 4.3

Lemma 4.3 (Upper-Bounding the Top- k Deferral Loss). *Let $x \in \mathcal{X}$ be an input, and $k \leq |\mathcal{A}|$ the size of the rejector set. Then, the top- k deferral loss satisfies:*

$$\ell_{\text{def},k}(R_k(x), a(x), z) \leq \sum_{j=0}^J \tau_j(a(x), z) \Phi_{01}^u(r, x, j) - (J - k) \sum_{j=0}^J c_j(a_j(x), z).$$

Proof. We establish an upper bound on the top- k deferral loss, which involves the multi-class classification loss Φ_{01}^u . First, we recall the definition of the top- k deferral loss:

$$\ell_{\text{def},k}(R_k(x), a(x), z) = \sum_{j=0}^J c_j(a_j(x), z) \mathbf{1}_{j \in R_k(x)}. \quad (9)$$

To facilitate the derivation of a surrogate top- k loss, we explicitly express the top- k deferral loss in terms of the top- k classification loss ℓ_k .

Given the rejector set $R_k(x) = \{r_{[0]_r^\downarrow}(x), \dots, r_{[k-1]_r^\downarrow}(x)\}$, we express the indicator function as

$$\mathbf{1}_{j \in R_k(x)} = \sum_{i=0}^{k-1} \mathbf{1}_{r_{[i]_r^\downarrow}(x)=j}, \quad (10)$$

where we use the fact that the elements of $R_k(x)$ are distinct. We further decompose this expression:

$$\mathbf{1}_{j \in R_k(x)} = \sum_{i=0}^{k-1} \left(\sum_{q=0}^J \mathbf{1}_{r_{[i]_r^\downarrow}(x) \neq q} \mathbf{1}_{q \neq j} - (J - 1) \right). \quad (11)$$

Rearranging, we obtain

$$\mathbf{1}_{j \in R_k(x)} = \sum_{i=0}^{k-1} \sum_{q=0}^J \mathbf{1}_{r_{[i]_r^\downarrow}(x) \neq q} \mathbf{1}_{q \neq j} - k(J - 1). \quad (12)$$

Substituting this into the loss expression, we derive

$$\begin{aligned} \ell_{\text{def},k}(R_k(x), a(x), z) &= \sum_{j=0}^J c_j(a_j(x), z) \left(\sum_{i=0}^{k-1} \sum_{q=0}^J \mathbf{1}_{r_{[i]_r^\downarrow}(x) \neq q} \mathbf{1}_{q \neq j} - k(J - 1) \right) \\ &= \sum_{q=0}^J \sum_{i=0}^{k-1} \left(\sum_{j=0}^J c_j(a_j(x), z) \mathbf{1}_{q \neq j} \right) \mathbf{1}_{r_{[i]_r^\downarrow}(x) \neq q} - k(J - 1) \sum_{j=0}^J c_j(a_j(x), z). \end{aligned} \quad (13)$$

Defining $\tau_q(a(x), z) := \sum_{j=0}^J c_j(a_j(x), z) \mathbf{1}_{q \neq j}$, we rewrite the loss as

$$\ell_{\text{def},k}(R_k(x), a(x), z) = \sum_{q=0}^J \sum_{i=0}^{k-1} \tau_q(a(x), z) \mathbf{1}_{r_{[i]_r^\downarrow}(x) \neq q} - k(J - 1) \sum_{j=0}^J c_j(a_j(x), z). \quad (14)$$

Further simplification yields

$$\ell_{\text{def},k}(R_k(x), a(x), z) = \sum_{j=0}^J \tau_j(a(x), z) \sum_{i=0}^{k-1} \mathbf{1}_{r_{[i]_r^\downarrow}(x) \neq j} - k(J - 1) \sum_{j=0}^J c_j(a_j(x), z). \quad (15)$$

We now establish the expression for the sum $\sum_{i=0}^{k-1} \mathbf{1}_{r_{[i]_r^\downarrow}(x) \neq j}$. Given that each $r_{[i]_r^\downarrow}(x)$ is unique, we derive

$$\sum_{i=0}^{k-1} \mathbf{1}_{r_{[i]_r^\downarrow}(x) \neq j} = (k - 1) \mathbf{1}_{j \in R_k(x)} + k \mathbf{1}_{j \notin R_k(x)}. \quad (16)$$

This leads to

$$\begin{aligned}
\ell_{\text{def},k}(R_k(x), a(x), z) &= \sum_{j=0}^J \tau_j(a(x), z) \left((k-1) + 1_{j \notin R_k(x)} \right) - k(J-1) \sum_{j=0}^J c_j(a_j(x), z) \\
&= \sum_{j=0}^J \tau_j(a(x), z) 1_{j \notin R_k(x)} + (k-1)J \sum_{j=0}^J c_j(a_j(x), z) - k(J-1) \sum_{j=0}^J c_j(a_j(x), z) \\
&= \sum_{j=0}^J \tau_j(a(x), z) 1_{j \notin R_k(x)} - (J-k) \sum_{j=0}^J c_j(a_j(x), z) \\
&= \sum_{j=0}^J \tau_j(a(x), z) \ell_k(R_k(x), j) - (J-k) \sum_{j=0}^J c_j(a_j(x), z)
\end{aligned} \tag{17}$$

This loss exactly coincides with the usual L2D loss (Narasimhan et al., 2022; Mao et al., 2023a, 2024b; Montreuil et al., 2024) by setting $k = 1$. Finally, utilizing the fact that $\Phi_{01}^u \geq \ell_k$ (Lapin et al., 2015; Cortes et al., 2024), we obtain the upper bound

$$\ell_{\text{def},k}(R_k(x), a(x), z) \leq \sum_{j=0}^J \tau_j(a(x), z) \Phi_{01}^u(r, x, j) - (J-k) \sum_{j=0}^J c_j(a_j(x), z). \tag{18}$$

We have proven an upper bound on $\ell_{\text{def},k}$. \square

A.9 Proof Corollary 4.4

Corollary 4.4 (Surrogates for the Top- k Deferral Loss). *Let $x \in \mathcal{X}$ be an input. The surrogates for the top- k deferral loss are defined as*

$$\Phi_{\text{def},k}^u(r, a(x), x, z) = \sum_{j=0}^J \tau_j(a(x), z) \Phi_{01}^u(r, x, j),$$

whose minimization is notably independent of the cardinality parameter k .

Proof. We begin with the previously established upper bound:

$$\ell_{\text{def},k}(R_k(x), a(x), z) \leq \sum_{j=0}^J \tau_j(a(x), z) \Phi_{01}^u(r, x, j) - (J-k) \sum_{j=0}^J c_j(a_j(x), z). \tag{19}$$

Since J and k are fixed parameters, and costs c_j do not depend on r , the final surrogate loss does not necessarily need to retain the last term, as it does not affect the optimization over r . Dropping this term, we define the surrogate for the top- k deferral loss as:

$$\Phi_{\text{def},k}^u(r, a(x), x, z) = \sum_{j=0}^J \tau_j(a(x), z) \Phi_{01}^u(r, x, j). \tag{20}$$

This completes the proof. \square

A.10 Proof Lemma 4.5

Lemma 4.5 (Bayes-optimal Rejector Set). *For a given query $x \in \mathcal{X}$, the Bayes-optimal rejector set $R_k^B(x)$ is defined as the subset of k agents with the lowest expected costs, ordered in increasing cost:*

$$R_k^B(x) = \arg \min_{\substack{R_k(x) \subseteq \mathcal{A} \\ |R_k(x)|=k}} \sum_{j \in R_k(x)} \bar{c}_j^*(a_j(x), z) = \{[0]_{\bar{c}^*}^\dagger, [1]_{\bar{c}^*}^\dagger, \dots, [k-1]_{\bar{c}^*}^\dagger\},$$

where the ordering satisfying $\forall j, j' \in R_k^B(x), j < j' \implies \bar{c}_j^*(a_j(x), z) \leq \bar{c}_{j'}^*(a_{j'}(x), z)$.

Proof. To simplify notation, define the expected costs and the optimal expected costs

$$\bar{c}(a(x), z) = \mathbb{E}_{z|x}[v(a(x), z)] \quad \text{and} \quad \bar{c}^*(x, y) = \inf_{g \in \mathcal{G}} \bar{c}(a(x), z). \quad (21)$$

Therefore, if $a(x) \neq g(x)$, we have that $\bar{c}^*(a(x), z) = \bar{c}(a(x), z)$.

Let $R_k(x) \subseteq \mathcal{A}$ be a set of k agents. The conditional risk of the top- k deferral loss is then

$$\mathcal{C}_{\ell_{\text{def}}, k}(r, g, x) = \mathbb{E}_{z|x}[\ell_{\text{def}, k}(R_k(x), a(x), x, z)] = \sum_{j=0}^J \bar{c}_j(a_j(x), z) 1_{j \in R_k(x)}, \quad (22)$$

where each \bar{c}_j is the expectation (over $z \mid x$) of c_j . In classification, we would have $y \mid x$, in regression $t \mid x$.

The *Bayes-optimal* conditional risk is

$$\mathcal{C}_{\ell_{\text{def}}, k}^B(\mathcal{R}, \mathcal{G}, x) = \inf_{g \in \mathcal{G}, r \in \mathcal{R}} \mathcal{C}_{\ell_{\text{def}}, k}(r, g, x) = \inf_{r \in \mathcal{R}} \sum_{j=0}^J \bar{c}_j^*(a_j(x), z) 1_{j \in R_k(x)}, \quad (23)$$

where \bar{c}_j^* denotes the optimal expected cost for agent j . Minimizing this sum by choosing exactly k terms is equivalent to picking the k smallest values among $\{\bar{c}_j^* : 0 \leq j \leq J\}$. Sorting them in ascending order,

$$\bar{c}_{[0]_{\bar{c}^*}}^*(a_{[0]_{\bar{c}^*}}(x), z) \leq \bar{c}_{[1]_{\bar{c}^*}}^*(a_{[1]_{\bar{c}^*}}(x), z) \leq \dots \leq \bar{c}_{[J]_{\bar{c}^*}}^*(a_{[J]_{\bar{c}^*}}(x), z), \quad (24)$$

the Bayes-optimal conditional risk becomes

$$\mathcal{C}_{\ell_{\text{def}}, k}^B(\mathcal{R}, \mathcal{G}, x) = \sum_{i=0}^{k-1} \bar{c}_{[i]_{\bar{c}^*}}^*(a_{[i]_{\bar{c}^*}}(x), z). \quad (25)$$

Consequently, the rejector set $R_k^B(x)$ that achieves this minimum is

$$R_k^B(x) = \arg \min_{\substack{R_k(x) \subseteq \mathcal{A} \\ |R_k(x)|=k}} \sum_{j \in R_k(x)} \bar{c}_j^*(a_j(x), z) = \{[0]_{\bar{c}^*}^\uparrow, [1]_{\bar{c}^*}^\uparrow, \dots, [k-1]_{\bar{c}^*}^\uparrow\}, \quad (26)$$

meaning $R_k^B(x)$ selects the k agents with the lowest optimal expected costs.

We have proven the desired result. \square

Remark 4. In the special case $k = 1$, this choice reduces to

$$\mathcal{C}_{\ell_{\text{def}}, 1}^B(\mathcal{R}, \mathcal{G}, x) = \min_{j \in \mathcal{A}} \bar{c}_j^*(a_j(x), z) = \bar{c}_{[0]_{\bar{c}^*}}^*(a_{[0]_{\bar{c}^*}}(x), z), \quad (27)$$

matching the usual L2D Bayes-conditional risk from (Mao et al., 2023a, 2024b; Montreuil et al., 2024).

For instance, suppose the optimal expected costs are:

$$\bar{c}_0^*(g(x), z) = 4, \quad \bar{c}_1^*(m_1(x), z) = 2, \quad \bar{c}_2^*(m_2(x), z) = 1. \quad (28)$$

Here, agent 2 has the lowest optimal expected cost, followed by agent 1, and then agent 0. Applying the Bayes-optimal selection:

For $k = 1$:

$$R_1^B(x) = \{2\}, \quad (29)$$

since agent 2 has the lowest cost.

For $k = 2$:

$$R_2^B(x) = \{2, 1\}, \quad (30)$$

as agents 2 and 1 are the two most cost-efficient choices.

For $k = 3$:

$$R_3^B(x) = \{2, 1, 0\}. \quad (31)$$

In this case, the rejector set is ordered as $\{2, 1, 0\}$, meaning that the system selects the most cost-efficient agents in decreasing order of efficiency.

A.11 Proof Theorem 4.6

First, we prove an intermediate Lemma.

Lemma A.7 (Consistency of a Top- k Loss). *A surrogate loss function Φ_{01}^u is said to be \mathcal{R} -consistent with respect to the top- k loss ℓ_k if, for any $r \in \mathcal{R}$, there exists a concave, increasing, and non-negative function $\Gamma^u : \mathbb{R}^+ \rightarrow \mathbb{R}^+$ such that:*

$$\sum_{j \in \mathcal{A}} p_j \mathbb{1}_{j \notin R_k(x)} - \inf_{r \in \mathcal{R}} \sum_{j \in \mathcal{A}} p_j \mathbb{1}_{j \notin R_k(x)} \leq \Gamma^u \left(\sum_{j \in \mathcal{A}} p_j \Phi_{01}^u(r, x, j) - \inf_{r \in \mathcal{R}} \sum_{j \in \mathcal{A}} p_j \Phi_{01}^u(r, x, j) \right), \quad (32)$$

where $p \in \Delta^{|\mathcal{A}|}$ denotes a probability distribution over the set \mathcal{A} .

Proof. Assuming the following inequality holds:

$$\sum_{j \in \mathcal{A}} p_j \mathbb{1}_{j \notin R_k(x)} - \inf_{r \in \mathcal{R}} \sum_{j \in \mathcal{A}} p_j \mathbb{1}_{j \notin R_k(x)} \leq \Gamma^u \left(\sum_{j \in \mathcal{A}} p_j \Phi_{01}^u(r, x, j) - \inf_{r \in \mathcal{R}} \sum_{j \in \mathcal{A}} p_j \Phi_{01}^u(r, x, j) \right), \quad (33)$$

we identify the corresponding conditional risks for a distribution $p \in \Delta^{|\mathcal{A}|}$ as introduced by [Awasthi et al. \(2022\)](#):

$$\mathcal{C}_{\ell_k}(r, x) - \inf_{r \in \mathcal{R}} \mathcal{C}_{\ell_k}(r, x) \leq \Gamma^u \left(\mathcal{C}_{\Phi_{01}^u}(r, x) - \inf_{r \in \mathcal{R}} \mathcal{C}_{\Phi_{01}^u}(r, x) \right). \quad (34)$$

Using the definition from [Awasthi et al. \(2022\)](#), we express the expected conditional risk difference as:

$$\begin{aligned} \mathbb{E}_x[\Delta \mathcal{C}_{\ell_k}(r, x)] &= \mathbb{E}_x \left[\mathcal{C}_{\ell_k}(r, x) - \inf_{r \in \mathcal{R}} \mathcal{C}_{\ell_k}(r, x) \right] \\ &= \mathcal{E}_{\ell_k}(r) - \mathcal{E}_{\ell_k}^B(\mathcal{R}) - \mathcal{U}_{\ell_k}(\mathcal{R}). \end{aligned} \quad (35)$$

Consequently, we obtain:

$$\mathcal{C}_{\ell_k}(r, x) - \inf_{r \in \mathcal{R}} \mathcal{C}_{\ell_k}(r, x) \leq \Gamma^u \left(\mathcal{C}_{\Phi_{01}^u}(r, x) - \inf_{r \in \mathcal{G}} \mathcal{C}_{\Phi_{01}^u}(r, x) \right). \quad (36)$$

Applying the expectation and by the Jensen's inequality yields:

$$\begin{aligned} \mathbb{E}_x[\Delta \mathcal{C}_{\ell_k}(r, x)] &\leq \mathbb{E}_x \left[\Gamma^u \left(\mathcal{C}_{\Phi_{01}^u}(r, x) \right) \right] \\ \mathbb{E}_x[\Delta \mathcal{C}_{\ell_k}(r, x)] &\leq \Gamma^u \left(\mathbb{E}_x \left[\mathcal{C}_{\Phi_{01}^u}(r, x) \right] \right). \end{aligned} \quad (37)$$

Then,

$$\mathcal{E}_{\ell_k}(r) - \mathcal{E}_{\ell_k}^B(\mathcal{R}) - \mathcal{U}_{\ell_k}(\mathcal{R}) \leq \Gamma^u \left(\mathcal{E}_{\Phi_{01}^u}(r) - \mathcal{E}_{\Phi_{01}^u}^*(\mathcal{R}) - \mathcal{U}_{\Phi_{01}^u}(\mathcal{R}) \right). \quad (38)$$

This result implies that the surrogate loss Φ_{01}^u is \mathcal{R} -consistent with respect to the top- k loss ℓ_k , completing the proof. \square

Theorem 4.6 ($(\mathcal{R}, \mathcal{G})$ -Consistency Bound). *Let $x \in \mathcal{X}$, and consider a hypothesis class \mathcal{R} that is regular, complete, and symmetric, along with any distribution \mathcal{D} . Suppose the cross-entropy surrogate family is \mathcal{R} -consistent. Then, there exists a non-decreasing, non-negative, concave function $\Gamma^u : \mathbb{R}^+ \rightarrow \mathbb{R}^+$, associated with the top- k loss ℓ_k and any surrogate from the cross-entropy family parameterized with u , such that the following bound holds:*

$$\begin{aligned} \mathcal{E}_{\ell_{def,k}}(g, r) - \mathcal{E}_{\ell_{def,k}}^B(\mathcal{G}, \mathcal{R}) - \mathcal{U}_{\ell_{def,k}}(\mathcal{G}, \mathcal{R}) &\leq \tilde{\Gamma}^u \left(\mathcal{E}_{\Phi_{def,k}^u}(r) - \mathcal{E}_{\Phi_{def,k}^u}^*(\mathcal{R}) - \mathcal{U}_{\Phi_{def,k}^u}(\mathcal{R}) \right) \\ &\quad + \mathbb{E}_x \left[\bar{c}_0(g(x), z) - \inf_{g \in \mathcal{G}} \bar{c}_0(g(x), z) \right], \end{aligned}$$

where $\bar{c}_0(g(x), z) = \mathbb{E}_{z|x}[c_0(g(x), z)]$, $Q = \sum_{j=0}^J \mathbb{E}_{z|x}[\tau_j(a(x), z)]$, and $\tilde{\Gamma}^u(v) = Q\Gamma^u\left(\frac{v}{Q}\right)$.

Proof. We establish the consistency of the proposed top- k deferral surrogate by leveraging the results from Lemma 4.5 and its proof in A.10.

The conditional risk associated with the top- k deferral loss is given by:

$$\mathcal{C}_{\ell_{\text{def},k}}(r, g, x) = \sum_{j=0}^J \bar{c}_j(a_j(x), z) 1_{j \in R_k(x)}, \quad (39)$$

and the Bayes-optimal conditional risk is expressed as (see A.10):

$$\mathcal{C}_{\ell_{\text{def},k}}^B(\mathcal{R}, \mathcal{G}, x) = \sum_{i=0}^{k-1} \bar{c}_{[i]_{\bar{c}^*}}^*(a_{[i]_{\bar{c}^*}}(x), z). \quad (40)$$

The calibration gap is then given by:

$$\begin{aligned} \Delta \mathcal{C}_{\text{def},k}(r, x) &= \mathcal{C}_{\text{def},k}(r, x) - \mathcal{C}_{\text{def},k}^B(\mathcal{R}, x) \\ &= \sum_{j=0}^J \bar{c}_j(a_j(x), z) 1_{j \in R_k(x)} - \sum_{i=0}^{k-1} \bar{c}_{[i]_{\bar{c}^*}}^*(a_{[i]_{\bar{c}^*}}(x), z) \\ &= \sum_{j=0}^J \bar{c}_j(a_j(x), z) 1_{j \in R_k(x)} - \sum_{i=0}^{k-1} \bar{c}_{[i]_{\bar{c}}}^{\uparrow}(a_{[i]_{\bar{c}}}^{\uparrow}(x), z) \\ &\quad + \left(\sum_{i=0}^{k-1} \bar{c}_{[i]_{\bar{c}}}^{\uparrow}(a_{[i]_{\bar{c}}}^{\uparrow}(x), z) - \sum_{i=0}^{k-1} \bar{c}_{[i]_{\bar{c}^*}}^*(a_{[i]_{\bar{c}^*}}(x), z) \right). \end{aligned} \quad (41)$$

Observing that:

$$\sum_{i=0}^{k-1} \bar{c}_{[i]_{\bar{c}}}^{\uparrow}(a_{[i]_{\bar{c}}}^{\uparrow}(x), z) - \sum_{i=0}^{k-1} \bar{c}_{[i]_{\bar{c}^*}}^*(a_{[i]_{\bar{c}^*}}(x), z) \leq \bar{c}_0(g(x), z) - \bar{c}_0^*(g(x), z), \quad (42)$$

we rewrite the first term using the conditional risks:

$$\sum_{j=0}^J \bar{c}_j(a_j(x), z) 1_{j \in R_k(x)} - \sum_{i=0}^{k-1} \bar{c}_{[i]_{\bar{c}}}^{\uparrow}(a_{[i]_{\bar{c}}}^{\uparrow}(x), z) = \mathcal{C}_{\ell_{\text{def},k}}(r, x) - \inf_{r \in \mathcal{R}} \mathcal{C}_{\ell_{\text{def},k}}(r, x). \quad (43)$$

Using the explicit formulation of the top- k deferral loss in terms of the indicator function $1_{j \notin R_k(x)}$ (Equation 17), we obtain:

$$\mathcal{C}_{\ell_{\text{def},k}}(r, x) - \inf_{r \in \mathcal{R}} \mathcal{C}_{\ell_{\text{def},k}}(r, x) = \sum_{j=0}^J \bar{\tau}_j(a(x), z) 1_{j \notin R_k(x)} - \inf_{r \in \mathcal{R}} \sum_{j=0}^J \bar{\tau}_j(a(x), z) 1_{j \notin R_k(x)}. \quad (44)$$

Using the change of variable $p_j = \frac{\bar{\tau}_j}{Q}$ with $Q = \sum_{j=0}^J \bar{\tau}_j$, it follows that:

$$\mathcal{C}_{\ell_{\text{def},k}}(r, x) - \inf_{r \in \mathcal{R}} \mathcal{C}_{\ell_{\text{def},k}}(r, x) = Q \left(\sum_{j=0}^J p_j 1_{j \notin R_k(x)} - \inf_{r \in \mathcal{R}} \sum_{j=0}^J p_j 1_{j \notin R_k(x)} \right). \quad (45)$$

Since the surrogate losses Φ_{01}^u are consistent with the top- k loss, we apply Lemma A.7:

$$\begin{aligned} \mathcal{C}_{\ell_{\text{def},k}}(r, x) - \inf_{r \in \mathcal{R}} \mathcal{C}_{\ell_{\text{def},k}}(r, x) &\leq Q \Gamma^u \left(\sum_{j=0}^J p_j \Phi_{01}^u(r, x, j) - \inf_{r \in \mathcal{R}} \sum_{j=0}^J p_j \Phi_{01}^u(r, x, j) \right) \\ &= Q \Gamma^u \left(\frac{1}{Q} \left[\mathcal{C}_{\Phi_{\text{def},k}^u}(r, x) - \inf_{r \in \mathcal{R}} \mathcal{C}_{\Phi_{\text{def},k}^u}(r, x) \right] \right). \end{aligned} \quad (46)$$

Incorporating Equation (42), we obtain:

$$\Delta \mathcal{C}_{\text{def},k}(r, x) \leq Q\Gamma^u \left(\frac{1}{Q} \left[\mathcal{C}_{\Phi_{\text{def},k}^u}(r, x) - \inf_{r \in \mathcal{R}} \mathcal{C}_{\Phi_{\text{def},k}^u}(r, x) \right] \right) + \bar{c}_0(g(x), z) - \bar{c}_0^*(g(x), z). \quad (47)$$

Taking expectations and applying Jensen's inequality for the concave function Γ^u yields:

$$\begin{aligned} \mathcal{E}_{\ell_{\text{def},k}}(g, r) - \mathcal{E}_{\ell_{\text{def},k}^B}(\mathcal{G}, \mathcal{R}) - \mathcal{U}_{\ell_{\text{def},k}}(\mathcal{G}, \mathcal{R}) &\leq \tilde{\Gamma}^u \left(\mathcal{E}_{\Phi_{\text{def},k}^u}(r) - \mathcal{E}_{\Phi_{\text{def},k}^*}(\mathcal{R}) - \mathcal{U}_{\Phi_{\text{def},k}^u}(\mathcal{R}) \right) \\ &\quad + \mathbb{E}_x \left[\bar{c}_0(g(x), z) - \inf_{g \in \mathcal{G}} \bar{c}_0(g(x), z) \right], \end{aligned}$$

where $\tilde{\Gamma}^u(v) = Q\Gamma^u(v/Q)$.

For the cross-entropy surrogates, Cortes et al. (2024) derived inverse transformation.

$$\Gamma^{-1}(v)^u = \begin{cases} k(1 - \sqrt{1 - v^2}) & u = 0 \\ k \left(\frac{1+v}{2} \log[1+v] + \frac{1-v}{2} \log[1-v] \right) & u = 1 \\ \frac{k}{v|\mathcal{A}|^v} \left[\left(\frac{(1+v)^{\frac{1}{1-v}} + (1-v)^{\frac{1}{1-v}}}{2} \right)^{1-v} - 1 \right] & u \in (0, 1) \\ \frac{k}{|\mathcal{A}|} v & u = 2. \end{cases} \quad (48)$$

If we specify $u = 1$, this corresponds to the log-softmax surrogate.

We have shown the consistency of our novel formulation. \square

A.12 Proof Bayes-Optimal Cardinality Lemma A.8

Cortes et al. (2024) have demonstrated that the cardinality loss ℓ_{car} can be effectively minimized using cross-entropy surrogates Φ_{01}^u , guaranteeing \mathcal{S} -consistency. Leveraging this consistency along with the Bayes-optimal rejector set structure (Lemma 4.5), we obtain the following key result:

Lemma A.8 (Bayes-Optimal Cardinality). *For $x \in \mathcal{X}$ define*

$$s^B(x) := \arg \min_{v \in \mathcal{A}} \mathbb{E}_{z|x} \left[\ell_{\text{car}}(\hat{R}_{v+1}(x), v, a(x), z) \right].$$

The Bayes-optimal rejector therefore keeps the $s^B(x) + 1$ agents with the lowest Bayes-optimal risk:

$$\hat{R}_{s^B(x)+1}(x) = \hat{R}_k(x) \Big|_{k=s^B(x)+1}.$$

We provide the corresponding training procedure in Algorithm 2 and report the computational complexity for both training and inference in Section A.3. Lemma A.8, proven in Appendix A.12, implies that learning the Bayes-optimal cardinality yields the most cost-effective minimal rejector set. Due to established consistency results, our learned rejector set $\hat{R}_{s^*(x)+1}(x)$ with optimal number of agents $s^*(x) + 1$, effectively approximates the Bayes-optimal solution $\hat{R}_{s^B(x)+1}(x)$.

Remark 5. In Lemma A.6, we formally show that our *Top-k(x) Learning-to-Defer* framework strictly generalizes classical model cascades.

Lemma A.8 (Bayes-Optimal Cardinality). *For $x \in \mathcal{X}$ define*

$$s^B(x) := \arg \min_{v \in \mathcal{A}} \mathbb{E}_{z|x} \left[\ell_{\text{car}}(\hat{R}_{v+1}(x), v, a(x), z) \right].$$

The Bayes-optimal rejector therefore keeps the $s^B(x) + 1$ agents with the lowest Bayes-optimal risk:

$$\hat{R}_{s^B(x)+1}(x) = \hat{R}_k(x) \Big|_{k=s^B(x)+1}.$$

Proof. Recall first the Bayes-optimal rejector set:

$$R_k^B(x) = \arg \min_{\substack{R_k(x) \subseteq \mathcal{A} \\ |R_k(x)|=k}} \sum_{j \in R_k(x)} \bar{c}_j^*(a_j(x), z), \quad (49)$$

which selects those k agents in \mathcal{A} that minimize the sum of the optimal expected costs \bar{c}_j^* .

Next, define the *cardinality loss* ℓ_{car} and its conditional risk:

$$\mathcal{C}_{\ell_{\text{car}}}(s, x) = \mathbb{E}_{z|x} \left[\ell_{\text{car}}(R_{s(x)+1}(x), s(x), a(x), z) \right], \quad (50)$$

where $s(x) \in \mathcal{A}$ is a *selector* that assigns a number of agents $s(x) + 1$ to each input x . The corresponding Bayes-optimal conditional risk over all selectors $s \in \mathcal{S}$ is

$$\mathcal{C}_{\ell_{\text{car}}}^B(\mathcal{S}, x) = \min_{v \in \mathcal{A}} \mathbb{E}_{z|x} \left[\ell_{\text{car}}(R_{v+1}(x), v, a(x), z) \right]. \quad (51)$$

As a result, the *Bayes-optimal selector* $s^B(x)$ is exactly the function that solves

$$s^B(x) = \arg \min_{v \in \mathcal{A}} \mathbb{E}_{z|x} \left[\ell_{\text{car}}(R_{v+1}(x), v, a(x), z) \right], \quad (52)$$

Intuitively, for every x , we pick whichever cardinality $v + 1$ leads to the lowest conditional risk under ℓ_{car} .

Then, taking the top- $(s^B(x) + 1)$ agents leads to the following Bayes-optimal rejector set:

$$R_{s^B(x)+1}^B(x) = R_k^B(x) \Big|_{k=s^B(x)+1} \quad (53)$$

□

A.13 Choice of the metric d

The choice of the metric d in the cardinality loss depends on the application-specific objectives. Ties are resolved by selecting the agent with the smallest index. In the event of a tie between predicted classes (e.g., in majority or weighted voting), we select the class predicted by the first agent in the rejector set. For any $r \in \mathcal{R}$ and rejector set $R_{|A|}(x)$.

Classification Metrics for Cardinality Loss. In classification, common choices include:

- **Top- k Loss** A binary penalty is incurred when the true label y is not present in the prediction set:

$$d_{\text{top-}k}(R_{v+1}(x), v, a(x), y) = 1_{y \notin \{a_{[0]_r^\downarrow}(x), \dots, a_{[v]_r^\downarrow}(x)\}}.$$

- **Weighted Voting Loss.** Each agent is weighted according to a reliability score, typically derived from a softmax over the rejector scores $r(x, \cdot)$. The predicted label is obtained via weighted voting:

$$\hat{y} = \arg \max_{y \in \mathcal{Y}} \sum_{j \in R_{v+1}(x)} w_j \cdot 1_{a_j(x)=y}, \quad \text{with } w_j = \hat{p}(x, j) = \frac{\exp(r(x, j))}{\sum_{j'} \exp(r(x, j'))}.$$

The loss is defined as:

$$d_{\text{w-vl}}(R_{v+1}(x), v, a(x), y) = 1_{y \neq \hat{y}}.$$

- **Majority Voting Loss.** All agents contribute equally, and the predicted label is chosen by majority vote:

$$\hat{y} = \arg \max_{y \in \mathcal{Y}} \sum_{j \in R_{v+1}(x)} 1_{a_j(x)=y},$$

with the corresponding loss:

$$d_{\text{maj}}(R_{v+1}(x), v, a(x), y) = 1_{y \neq \hat{y}}.$$

Regression Metrics for Cardinality Loss. Let $\ell_{\text{reg}}(t, \hat{t}) \in \mathbb{R}^+$ denote a base regression loss (e.g., squared error or smooth L1). Common choices include:

- **Minimum Cost (Best Expert) Loss.** The error is measured using the prediction from the best-performing agent in the rejector set:

$$d_{\min}(R_{v+1}(x), v, a(x), t) = \min_{j \in R_{v+1}(x)} \ell_{\text{reg}}(a_j(x), t).$$

- **Weighted Average Prediction Loss.** Each agent is assigned a reliability weight based on a softmax over rejector scores $r(x, \cdot)$. The predicted output is a weighted average of agent predictions:

$$\hat{t} = \sum_{j \in R_{v+1}(x)} w_j \cdot a_j(x), \quad \text{with} \quad w_j = \frac{\exp(r(x, j))}{\sum_{j'} \exp(r(x, j'))},$$

and the loss is computed as:

$$d_{\text{w-avg}}(R_{v+1}(x), v, a(x), t) = \ell_{\text{reg}}(\hat{t}, t).$$

- **Uniform Average Prediction Loss.** Each agent in the rejector set contributes equally, and the final prediction is a simple average:

$$\hat{t} = \frac{1}{v+1} \sum_{j \in R_{v+1}(x)} a_j(x), \quad d_{\text{avg}}(R_{v+1}(x), v, a(x), t) = \ell_{\text{reg}}(\hat{t}, t).$$

A.14 Experiments

We compare our proposed *Top-k* and *Top-k(x)* L2D approaches against prior work (Narasimhan et al., 2022; Mao et al., 2023a, 2024b), as well as against random and oracle (optimal) baselines.

A.14.1 Datasets

CIFAR-100. CIFAR-100 is a widely used image classification benchmark consisting of 60,000 color images of size 32×32 , evenly distributed across 100 fine-grained object categories (Krizhevsky, 2009). Each class contains 600 examples, with 50,000 images for training and 10,000 for testing. The large number of visually similar categories makes this dataset a challenging benchmark for evaluating multi-agent decision systems. We follow the standard split and apply dataset-specific normalization.

SVHN. The Street View House Numbers (SVHN) dataset (Goodfellow et al., 2013) is a digit classification benchmark composed of over 600,000 RGB images of 32×32 pixels, extracted from real-world street scenes (non-commercial use only). It contains significant variability in digit scale, orientation, and background clutter. We use the standard split: 73,257 training and 26,032 test images.

California Housing. The California Housing dataset (Kelley Pace and Barry, 1997) is a regression benchmark based on the 1990 U.S. Census (CC0). It contains 20,640 instances, each representing a geographical block in California and described by eight real-valued features (e.g., median income, average occupancy). The target is the median house value in each block, measured in hundreds of thousands of dollars. We standardize all features and use an 80/20 train-test split.

A.14.2 Metrics

For classification tasks, we report accuracy under three evaluation rules. The *Top-k Accuracy* is defined as $\text{Acc}_{\text{top-}k} = \mathbb{E}_x[1 - d_{\text{top-}k}(x)]$, where the prediction is deemed correct if the true label y is included in the outputs of the queried agents. The *Weighted Voting Accuracy* is given by $\text{Acc}_{\text{w-vl}} = \mathbb{E}_x[1 - d_{\text{w-vl}}(x)]$, where agent predictions are aggregated via softmax-weighted voting. Finally, the *Majority Voting Accuracy* is defined as $\text{Acc}_{\text{maj}} = \mathbb{E}_x[1 - d_{\text{maj}}(x)]$, where all agents in the rejector set contribute equally.

For regression tasks, we report RMSE under three aggregation strategies. The *Minimum Cost RMSE* is defined as $\text{RMSE}_{\min} = \mathbb{E}_x[d_{\min}(x)]$, corresponding to the prediction from the best-performing

agent. The *Weighted Average Prediction RMSE* is given by $\text{RMSE}_{w\text{-avg}} = \mathbb{E}_x[d_{w\text{-avg}}(x)]$, using a softmax-weighted average of predictions. The *Uniform Average Prediction RMSE* is computed as $\text{RMSE}_{\text{avg}} = \mathbb{E}_x[d_{\text{avg}}(x)]$, using the unweighted mean of agent predictions.

In addition to performance, we also report two resource-sensitive metrics. The *expected budget* is defined as $\bar{\beta}(k) = \mathbb{E}_x \left[\sum_{j=0}^{k-1} \beta_{[j]_{\hat{r}}^{\downarrow}} \right]$, where β_j denotes the consultation cost of agent j , and $[j]_{\hat{r}}^{\downarrow}$ is the index of the j -th ranked agent by the learned rejector \hat{r} . The *expected number of queried agents* is given by $\bar{k} = \mathbb{E}_x[|R_k(x)|]$, where k is fixed for Top- k L2D and varies with x in the adaptive Top- $k(x)$ L2D setting. Additional implementation and evaluation details are provided in Appendix A.13.

A.14.3 General Settings for Top- k and Top- $k(x)$ L2D

For each dataset, we configure a pool of six agents with a predefined consultation cost vector $\beta = (0, 0.05, 0.045, 0.040, 0.035, 0.03)$ and uniform scaling factors $\alpha_j = 1$, resulting in the agent index set $\mathcal{A} = \{0, 1, \dots, 5\}$. While the exact cost values are not critical to the Learning-to-Defer framework, they are chosen to simulate realistic deployment scenarios in which agents incur different operational costs (Madras et al., 2018; Mozannar and Sontag, 2020; Verma et al., 2022). This heterogeneity reflects systems composed of lightweight and heavyweight models, or a mixture of automated and human decision-makers with varying accessibility. The allocation policy is trained to account for both the predictive accuracy and consultation cost of each agent, thereby optimizing the overall cost-performance trade-off. For surrogates, we use the log-softmax loss $\Phi_{01}^{u=1}(r, x, j) = -\log \left(\frac{e^{r(x,j)}}{\sum_{j' \in \mathcal{A}} e^{r(x,j')}} \right)$ as our multiclass classification surrogate.

To assess the sensitivity of the selector and its impact on agent cardinality, we conduct experiments using multiple instantiations of the metric d ; detailed formulations are provided in Section A.14.2. We additionally report results across a sweep of hyperparameters $\lambda \in \{1 \times 10^{-9}, 0.01, 0.05, 0.25, 0.5, 1, 1.5, \dots, 6.5\}$, which directly influence the learned number of agents $k = k(x)$. We choose to define the function $\xi(\cdot)$ as a linear function $\xi(v) = v$ and the log-softmax loss $\Phi_{01}^{u=1}(s, x, v) = -\log \left(\frac{e^{s(x,v)}}{\sum_{v' \in \mathcal{A}} e^{s(x,v')}} \right)$ as our multiclass classification surrogate. In the case of a tie, we break ties by selecting the first element according to a fixed ordering.

A.14.4 Reproducibility

All scripts and configurations are publicly available to facilitate reproducibility. We report both the mean and variance across four independent runs, with a fixed agent distribution. For random policies, results are averaged over fifty runs. All plots include error bars representing the mean and one standard deviation. Dataset-specific variability and additional implementation details are provided in the corresponding dataset sections.

A.14.5 Resources

All experiments were performed on an internal computing cluster using an NVIDIA A100 GPU with 40 GB of VRAM. For Top- $k(x)$ L2D, the average GPU memory usage was approximately 7.2 GB for SVHN, 7.0 GB for CIFAR-100, and 6.8 GB for California Housing. In comparison, Top- k L2D required less memory: 2.0 GB for both SVHN and CIFAR-100, and 1.41 GB for California Housing.

A.14.6 Results on California Housing.

Agent setting. We construct a pool of 6 regression agents, each trained on a predefined, spatially localized subset of the California Housing dataset. To simulate domain specialization, each agent is associated with a specific geographical region of California, reflecting scenarios in which real estate professionals possess localized expertise. The training regions are partially overlapping to introduce heterogeneity and ensure that no single agent has access to all regions, thereby creating a realistic setting for deferral and expert allocation.

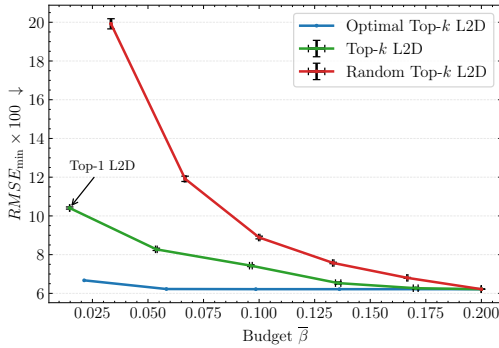
We train each agent using a multilayer perceptron (MLP) for 30 epochs with a batch size of 256, a learning rate of 1×10^{-3} , optimized using Adam. Model selection is based on the checkpoint achieving the lowest RMSE on the agent’s corresponding validation subset. We report the RMSE on the entire California validation set in table 1.

Table 1: RMSE $\times 100$ of each agent on the California validation set.

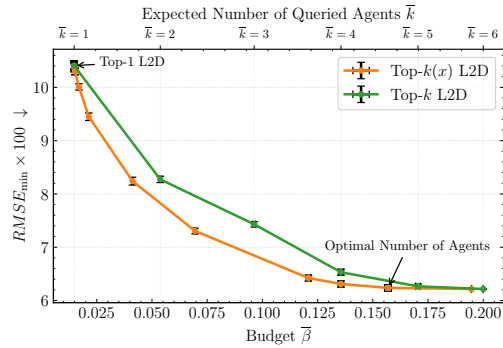
Agent	0	1	2	3	4	5
RMSE $\times 100$	21.97	15.72	31.81	16.20	27.06	40.26

Top- k L2D. We train a two-layer MLP following Algorithm 1. The rejector is trained for 100 epochs with a batch size of 256, a learning rate of 5×10^{-4} , using the Adam optimizer and a cosine learning rate scheduler. We select the checkpoint that achieves the lowest Top- k surrogate loss on the validation set, yielding the final rejector \hat{r} . We report Top- k L2D performance for each fixed value $k \in \mathcal{A}$.

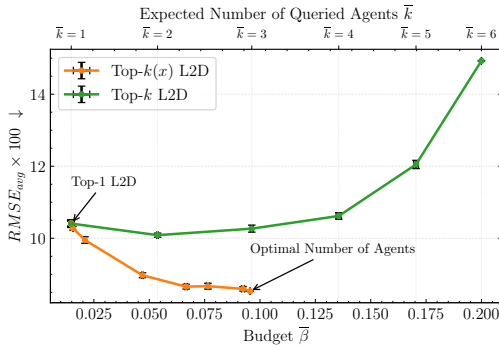
Top- $k(x)$ L2D. We train the selector using the same two-layer MLP architecture, following Algorithm 2. The selector is also trained for 100 epochs with a batch size of 256, a learning rate of 5×10^{-4} , using Adam and cosine scheduling. We conduct additional experiments using various instantiations of the metric d , as detailed in Section A.14.2.



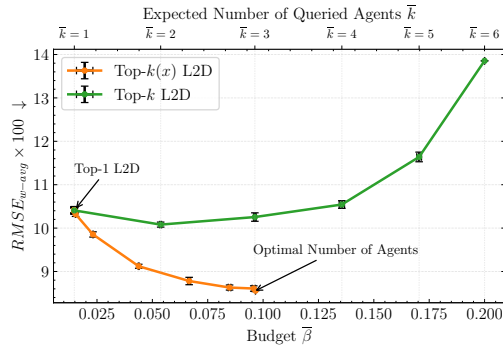
(a) Comparison with Random and Optimal Baselines: We compare Top- k L2D against random and oracle baselines using the $RMSE_{\min}$ metric defined in Section A.14.2. Our method consistently outperforms both baselines and extends the Top-1 L2D formulation introduced by Mao et al. (2024b).



(b) Comparison of Top- k L2D and Top- $k(x)$ L2D under $RMSE_{\min}$ metric. We report the $RMSE_{\min}$ metric, along with the budget and the expected number of queried agents. Across all budgets, Top- $k(x)$ consistently outperforms Top- k L2D by achieving lower error with fewer agents and reduced cost.



(c) Comparison of Top- k L2D and Top- $k(x)$ L2D under $RMSE_{\text{avg}}$ metric.



(d) Comparison of Top- k L2D and Top- $k(x)$ L2D under $RMSE_{w\text{-avg}}$ metric.

Figure 5: Results on the California dataset comparing Top- k and Top- $k(x)$ L2D across four evaluation metrics. Top- $k(x)$ consistently achieves superior performance across all trade-offs.

Performance Comparison. Figures 5, compare Top- k and Top- $k(x)$ L2D across multiple evaluation metrics and budget regimes. Top- k L2D consistently outperforms random baselines and closely

approaches the oracle (optimal) strategy under the RMSE_{\min} metric, validating the benefit of using different agents (Table 1).

In Figure 5b, $\text{Top-}k(x)$ achieves near-optimal performance (6.23) with a budget of $\bar{\beta} = 0.156$ and an expected number of agents $\bar{k} = 4.77$, whereas $\text{Top-}k$ requires the full budget $\bar{\beta} = 0.2$ and $\bar{k} = 6$ agents to reach a comparable score (6.21). This demonstrates the ability of $\text{Top-}k(x)$ to allocate resources more efficiently by querying only the necessary number of agents, in contrast to $\text{Top-}k$, which tends to over-allocate costly or redundant experts. Additionally, our approach outperforms the Top-1 L2D baseline (Mao et al., 2024b), confirming the limitations of single-agent deferral.

Figures 5c and 5d evaluate $\text{Top-}k$ and $\text{Top-}k(x)$ L2D under more restrictive metrics— RMSE_{avg} and $\text{RMSE}_{w\text{-avg}}$ —where performance is not necessarily monotonic in the number of queried agents. In these settings, consulting too many or overly expensive agents may degrade overall performance. $\text{Top-}k(x)$ consistently outperforms $\text{Top-}k$ by carefully adjusting the number of consulted agents. In both cases, it achieves optimal performance with a budget of only $\bar{\beta} = 0.095$, a level that $\text{Top-}k$ fails to reach. For example, in Figure 5c, $\text{Top-}k(x)$ achieves $\text{RMSE}_{\text{avg}} = 8.53$, compared to 10.08 for $\text{Top-}k$. Similar trends are observed under the weighted average metric (Figure 5d), where $\text{Top-}k(x)$ again outperforms $\text{Top-}k$, suggesting that incorporating rejector-derived weights w_j leads to more effective aggregation. This demonstrates that our $\text{Top-}k(x)$ L2D selectively chooses the appropriate agents—when necessary—to enhance the overall system performance.

A.14.7 Results on SVHN

Agent setting. We construct a pool of 6 convolutional neural networks (CNNs), each trained on a randomly sampled, partially overlapping subset of the SVHN dataset (20%). This setup simulates realistic settings where agents are trained on distinct data partitions due to privacy constraints or institutional data siloing. As a result, the agents exhibit heterogeneous predictive capabilities and error patterns.

Each agent is trained for 3 epochs using the Adam optimizer (Kingma and Ba, 2014), with a batch size of 64 and a learning rate of 1×10^{-3} . Model selection is performed based on the lowest loss on each agent’s respective validation subset. The table 2 below reports the classification accuracy of each trained agent, evaluated on a common held-out validation set:

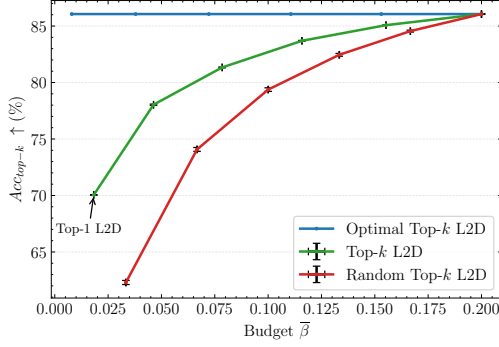
Table 2: Accuracy of each agent on the SVHN validation set.

Agent	0	1	2	3	4	5
Accuracy (%)	63.51	55.53	61.56	62.60	66.66	64.26

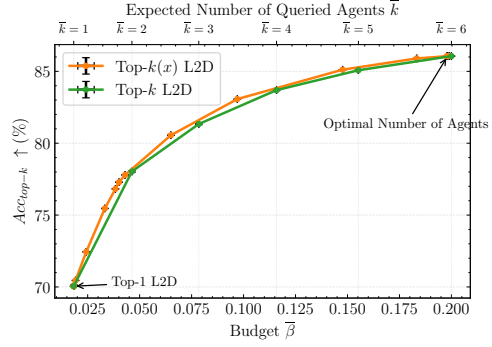
Top- k L2D. We train the rejector using a ResNet-4 architecture (He et al., 2016), following Algorithm 1. The model is trained for 50 epochs with a batch size of 256 and an initial learning rate of 1×10^{-2} , scheduled via cosine annealing. Optimization is performed using the Adam optimizer. We select the checkpoint that minimizes the Top- k surrogate loss on the validation set, yielding the final rejector \hat{r} . We report Top- k L2D performance for each fixed value $k \in \mathcal{A}$.

Top- $k(x)$ L2D. We reuse the trained rejector \hat{r} and follow Algorithm 2 to train a cardinality selector $s \in \mathcal{S}$. The selector is composed of a CLIP-based feature extractor (Radford et al., 2021) and a lightweight classification head. It is trained for 10 epochs with a batch size of 256, a learning rate of 1×10^{-3} , weight decay of 1×10^{-5} , and cosine learning rate scheduling. We use the AdamW optimizer (Loshchilov and Hutter, 2017) for optimization.

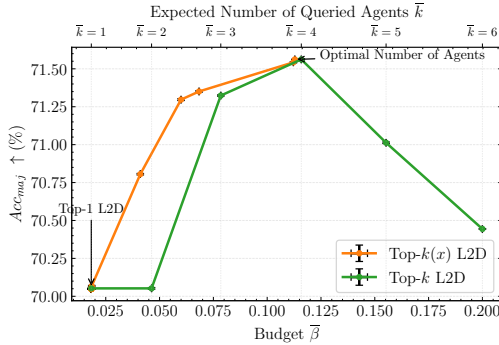
Performance Comparison. Figure 6 compares our $\text{Top-}k$ and $\text{Top-}k(x)$ L2D approaches against prior work (Narasimhan et al., 2022; Mao et al., 2023a), as well as oracle and random baselines. As shown in Figure 6a, querying multiple agents significantly improves performance, with both of our methods surpassing the Top-1 L2D baselines (Narasimhan et al., 2022; Mao et al., 2023a). Moreover, our learned deferral strategies consistently outperform the random L2D baseline, underscoring the effectiveness of our allocation policy in routing queries to appropriate agents. In Figure 6b, Top-



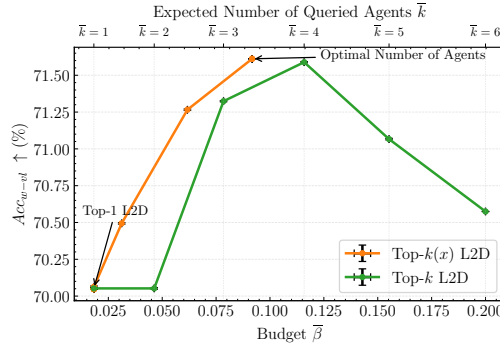
(a) Comparison with Random and Optimal baselines using $\text{Acc}_{\text{top-}k}$.



(b) $\text{Top-}k(x)$ vs. $\text{Top-}k$ L2D on $\text{Acc}_{\text{top-}k}$.



(c) Performance under Acc_{maj} metric.



(d) Performance under Acc_{w-v1} metric.

Figure 6: Comparison of $\text{Top-}k$ and $\text{Top-}k(x)$ L2D across four accuracy metrics on SVHN. $\text{Top-}k(x)$ achieves better budget-accuracy trade-offs across all settings.

$k(x)$ L2D consistently outperforms $\text{Top-}k$ L2D, achieving better accuracy under the same budget constraints.

For more restrictive metrics, Figures 6c and 6d show that $\text{Top-}k(x)$ achieves notably stronger performance, particularly in the low-budget regime. For example, in Figure 6c, at a budget of $\beta = 0.41$, $\text{Top-}k(x)$ attains $\text{Acc}_{\text{maj}} = 70.81$, compared to $\text{Acc}_{\text{maj}} = 70.05$ for $\text{Top-}k$. This performance gap widens further at smaller budgets. Both figures also highlight that querying too many agents may degrade accuracy due to the inclusion of low-quality predictions. In contrast, $\text{Top-}k(x)$ identifies a better trade-off, reaching up to $\text{Acc}_{\text{maj}} = 71.56$ under majority voting and $\text{Acc}_{w-v1} = 71.59$ with weighted voting. As in the California Housing experiment, weighted voting outperforms majority voting, suggesting that leveraging rejector-derived weights improves overall decision quality.

A.14.8 Results on CIFAR100.

Agent setting. We construct a pool of 6 agents. We train a main model (agent 0) using a ResNet-4 (He et al., 2016) for 50 epochs, a batch size of 256, the Adam Optimizer (Kingma and Ba, 2014) and select the checkpoints with the lower validation loss. We synthetically create 5 experts with strong overlapped knowledge. We assign experts to classes for which they have the probability to be correct reaching $p = 0.94$ and uniform in non-assigned classes. Typically, we assign 55 classes to each experts. We report in the table 3 the accuracy of each agents on the validation set.

Top- k L2D. We train the rejector model using a ResNet-4 architecture (He et al., 2016), following the procedure described in Algorithm 1. The model is optimized using Adam with a batch size of 2048, an initial learning rate of 1×10^{-3} , and cosine annealing over 200 training epochs. We select the checkpoint that minimizes the Top- k surrogate loss on the validation set, resulting in the final rejector \hat{r} . We report Top- k L2D performance for each fixed value $k \in \mathcal{A}$.

Table 3: Accuracy of each agent on the CIFAR100 validation set.

Agent	0	1	2	3	4	5
Accuracy (%)	59.74	51.96	52.58	52.21	52.32	52.25

Top- $k(x)$ L2D. We reuse the learned rejector \hat{r} and train a cardinality selector $s \in \mathcal{S}$ as described in Algorithm 2. The selector is composed of a CLIP-based feature extractor (Radford et al., 2021) and a lightweight classification head. It is trained using the AdamW optimizer (Loshchilov and Hutter, 2017) with a batch size of 128, a learning rate of 1×10^{-3} , weight decay of 1×10^{-5} , and cosine learning rate scheduling over 15 epochs. To evaluate performance under different decision rules, we conduct experiments using multiple instantiations of the metric d ; detailed definitions and evaluation protocols are provided in Section A.14.2.

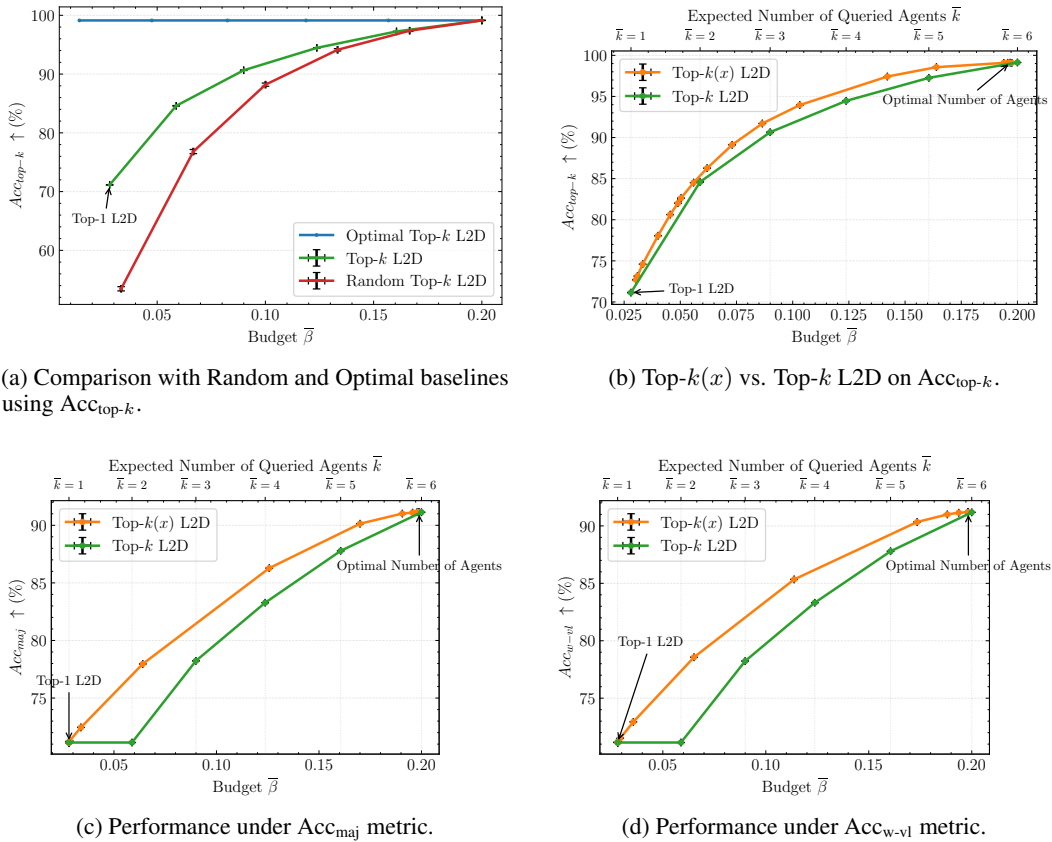


Figure 7: Comparison of Top- k and Top- $k(x)$ L2D across four accuracy metrics on CIFAR100. Top- $k(x)$ achieves better budget-accuracy trade-offs across all settings.

Performance Comparison. Figure 7b shows that Top- k L2D outperforms random query allocation, validating the benefit of learned deferral policies. As shown in Figure 7a, Top- $k(x)$ further improves performance over Top- k by adaptively selecting the number of agents per query. In Figures 7c and 7d, Top- $k(x)$ consistently yields higher accuracy across all budget levels, achieving significant gains over fixed- k strategies.

Notably, unlike in other datasets, querying additional agents in this setting does not degrade performance. This is due to the absence of low-quality agents: each agent predicts correctly with high probability (at least 94%) on its assigned class subset. As a result, aggregating predictions from multiple agents improves accuracy by selectively querying them.

Nevertheless, $\text{Top-}k(x)$ remains advantageous due to the overlap between agents and their differing consultation costs. When several agents are likely to produce correct predictions, it is preferable to defer to the less costly one. By exploiting this flexibility, $\text{Top-}k(x)$ achieves a large performance improvements over $\text{Top-}k$ L2D while also reducing the overall budget.

A.15 Limitations

Our approach is currently limited to the two-stage setting, where the main model g is trained offline. Extending the framework to a one-stage setting—where the rejector and predictive model are learned jointly—would require a substantially different formulation and a careful theoretical treatment, which we leave as an important direction for future work. Additionally, the cardinality loss defined in Definition 4.7 implicitly assumes uniform scaling factors $\alpha_j = 1$ across agents. While this restricts expressiveness, we believe it is not a major practical limitation, as uniform scaling is a common assumption in prior Learning-to-Defer work. Furthermore, we do not evaluate our method using human expert annotations or real-world expert datasets. While such data would add realism, it offers limited flexibility for simulating practical scenarios such as cost-sensitive allocation, input-dependent specialization, or performance-controlled diversity. This lack of flexibility makes real-world expert datasets less suitable for controlled experimentation. We view this as a broader limitation of current Learning-to-Defer paradigms, which generally assume access to a static, predefined set of experts with offline predictions or annotations, and lack support for interactive or dynamic querying. Aside from these points, our method inherits standard constraints present in most L2D frameworks, including reliance on expert labels, offline availability of expert predictions, and the assumption that expert behaviors are fixed during training and evaluation.

NeurIPS Paper Checklist

1. Claims

Question: Do the main claims made in the abstract and introduction accurately reflect the paper's contributions and scope?

Answer: [\[Yes\]](#)

Justification: We clearly state our main contributions in both the *Abstract* and *Introduction* (Section 1). The generalization of the Two-Stage L2D framework is presented in Section 4.1, and our theoretical guarantees are detailed in Section 4.3. Furthermore, we show that model cascades arise as a special case of our approach in Appendices A.5 and A.5.3. We support our theoretical work with experiments in Section 6.

Guidelines:

- The answer NA means that the abstract and introduction do not include the claims made in the paper.
- The abstract and/or introduction should clearly state the claims made, including the contributions made in the paper and important assumptions and limitations. A No or NA answer to this question will not be perceived well by the reviewers.
- The claims made should match theoretical and experimental results, and reflect how much the results can be expected to generalize to other settings.
- It is fine to include aspirational goals as motivation as long as it is clear that these goals are not attained by the paper.

2. Limitations

Question: Does the paper discuss the limitations of the work performed by the authors?

Answer: [\[Yes\]](#)

Justification: Yes, we have included limitations we have identified. We have deferred this in Appendix A.15.

Guidelines:

- The answer NA means that the paper has no limitation while the answer No means that the paper has limitations, but those are not discussed in the paper.
- The authors are encouraged to create a separate "Limitations" section in their paper.
- The paper should point out any strong assumptions and how robust the results are to violations of these assumptions (e.g., independence assumptions, noiseless settings, model well-specification, asymptotic approximations only holding locally). The authors should reflect on how these assumptions might be violated in practice and what the implications would be.
- The authors should reflect on the scope of the claims made, e.g., if the approach was only tested on a few datasets or with a few runs. In general, empirical results often depend on implicit assumptions, which should be articulated.
- The authors should reflect on the factors that influence the performance of the approach. For example, a facial recognition algorithm may perform poorly when image resolution is low or images are taken in low lighting. Or a speech-to-text system might not be used reliably to provide closed captions for online lectures because it fails to handle technical jargon.
- The authors should discuss the computational efficiency of the proposed algorithms and how they scale with dataset size.
- If applicable, the authors should discuss possible limitations of their approach to address problems of privacy and fairness.
- While the authors might fear that complete honesty about limitations might be used by reviewers as grounds for rejection, a worse outcome might be that reviewers discover limitations that aren't acknowledged in the paper. The authors should use their best judgment and recognize that individual actions in favor of transparency play an important role in developing norms that preserve the integrity of the community. Reviewers will be specifically instructed to not penalize honesty concerning limitations.

3. Theory Conclusion, assumptions and proofs

Question: For each theoretical result, does the paper provide the full set of assumptions and a complete (and correct) proof?

Answer: [Yes]

Justification: For each notion introduced, we clearly state the assumptions used directly above the corresponding claim when necessary. Detailed proofs for all stated lemmas, theorems, and corollaries are provided in Appendix A. For ease of navigation, we refer the reader to the Table of Contents.

Guidelines:

- The answer NA means that the paper does not include theoretical results.
- All the theorems, formulas, and proofs in the paper should be numbered and cross-referenced.
- All assumptions should be clearly stated or referenced in the statement of any theorems.
- The proofs can either appear in the main paper or the supplemental material, but if they appear in the supplemental material, the authors are encouraged to provide a short proof sketch to provide intuition.
- Inversely, any informal proof provided in the core of the paper should be complemented by formal proofs provided in appendix or supplemental material.
- Theorems and Lemmas that the proof relies upon should be properly referenced.

4. Experimental result reproducibility

Question: Does the paper fully disclose all the information needed to reproduce the main experimental results of the paper to the extent that it affects the main claims and/or conclusions of the paper (regardless of whether the code and data are provided or not)?

Answer: [Yes]

Justification: In the main body of the paper, we present experiments on the California Housing dataset. Additional results on CIFAR-100 and SVHN are provided in Appendix A.14. Appendix A.14 also includes detailed descriptions of the datasets, formal definitions of the evaluation metrics, and training configurations for all baselines. Furthermore, we provide the complete algorithms for both Top- k and Top- $k(x)$ L2D in Appendix A.1, and we make our code publicly available to facilitate reproducibility.

Guidelines:

- The answer NA means that the paper does not include experiments.
- If the paper includes experiments, a No answer to this question will not be perceived well by the reviewers: Making the paper reproducible is important, regardless of whether the code and data are provided or not.
- If the contribution is a dataset and/or model, the authors should describe the steps taken to make their results reproducible or verifiable.
- Depending on the contribution, reproducibility can be accomplished in various ways. For example, if the contribution is a novel architecture, describing the architecture fully might suffice, or if the contribution is a specific model and empirical evaluation, it may be necessary to either make it possible for others to replicate the model with the same dataset, or provide access to the model. In general, releasing code and data is often one good way to accomplish this, but reproducibility can also be provided via detailed instructions for how to replicate the results, access to a hosted model (e.g., in the case of a large language model), releasing of a model checkpoint, or other means that are appropriate to the research performed.
- While NeurIPS does not require releasing code, the conference does require all submissions to provide some reasonable avenue for reproducibility, which may depend on the nature of the contribution. For example
 - (a) If the contribution is primarily a new algorithm, the paper should make it clear how to reproduce that algorithm.
 - (b) If the contribution is primarily a new model architecture, the paper should describe the architecture clearly and fully.

- (c) If the contribution is a new model (e.g., a large language model), then there should either be a way to access this model for reproducing the results or a way to reproduce the model (e.g., with an open-source dataset or instructions for how to construct the dataset).
- (d) We recognize that reproducibility may be tricky in some cases, in which case authors are welcome to describe the particular way they provide for reproducibility. In the case of closed-source models, it may be that access to the model is limited in some way (e.g., to registered users), but it should be possible for other researchers to have some path to reproducing or verifying the results.

5. Open access to data and code

Question: Does the paper provide open access to the data and code, with sufficient instructions to faithfully reproduce the main experimental results, as described in supplemental material?

Answer: [Yes]

Justification: We make our code publicly available, along with detailed instructions to facilitate reproducibility.

Guidelines:

- The answer NA means that paper does not include experiments requiring code.
- Please see the NeurIPS code and data submission guidelines (<https://nips.cc/public/guides/CodeSubmissionPolicy>) for more details.
- While we encourage the release of code and data, we understand that this might not be possible, so “No” is an acceptable answer. Papers cannot be rejected simply for not including code, unless this is central to the contribution (e.g., for a new open-source benchmark).
- The instructions should contain the exact command and environment needed to run to reproduce the results. See the NeurIPS code and data submission guidelines (<https://nips.cc/public/guides/CodeSubmissionPolicy>) for more details.
- The authors should provide instructions on data access and preparation, including how to access the raw data, preprocessed data, intermediate data, and generated data, etc.
- The authors should provide scripts to reproduce all experimental results for the new proposed method and baselines. If only a subset of experiments are reproducible, they should state which ones are omitted from the script and why.
- At submission time, to preserve anonymity, the authors should release anonymized versions (if applicable).
- Providing as much information as possible in supplemental material (appended to the paper) is recommended, but including URLs to data and code is permitted.

6. Experimental setting/details

Question: Does the paper specify all the training and test details (e.g., data splits, hyperparameters, how they were chosen, type of optimizer, etc.) necessary to understand the results?

Answer: [Yes]

Justification: All training details, including hyperparameters and optimization settings for each experiment, are provided in Appendix A.14.

Guidelines:

- The answer NA means that the paper does not include experiments.
- The experimental setting should be presented in the core of the paper to a level of detail that is necessary to appreciate the results and make sense of them.
- The full details can be provided either with the code, in appendix, or as supplemental material.

7. Experiment statistical significance

Question: Does the paper report error bars suitably and correctly defined or other appropriate information about the statistical significance of the experiments?

Answer: [Yes]

Justification: All relevant details are provided in Appendix A.14.4, where we describe how error bars were computed and how statistical significance was assessed.

Guidelines:

- The answer NA means that the paper does not include experiments.
- The authors should answer "Yes" if the results are accompanied by error bars, confidence intervals, or statistical significance tests, at least for the experiments that support the main claims of the paper.
- The factors of variability that the error bars are capturing should be clearly stated (for example, train/test split, initialization, random drawing of some parameter, or overall run with given experimental conditions).
- The method for calculating the error bars should be explained (closed form formula, call to a library function, bootstrap, etc.)
- The assumptions made should be given (e.g., Normally distributed errors).
- It should be clear whether the error bar is the standard deviation or the standard error of the mean.
- It is OK to report 1-sigma error bars, but one should state it. The authors should preferably report a 2-sigma error bar than state that they have a 96% CI, if the hypothesis of Normality of errors is not verified.
- For asymmetric distributions, the authors should be careful not to show in tables or figures symmetric error bars that would yield results that are out of range (e.g. negative error rates).
- If error bars are reported in tables or plots, The authors should explain in the text how they were calculated and reference the corresponding figures or tables in the text.

8. Experiments compute resources

Question: For each experiment, does the paper provide sufficient information on the computer resources (type of compute workers, memory, time of execution) needed to reproduce the experiments?

Answer: [Yes]

Justification: Details on the computational resources used are provided in Appendix A.14.5.

Guidelines:

- The answer NA means that the paper does not include experiments.
- The paper should indicate the type of compute workers CPU or GPU, internal cluster, or cloud provider, including relevant memory and storage.
- The paper should provide the amount of compute required for each of the individual experimental runs as well as estimate the total compute.
- The paper should disclose whether the full research project required more compute than the experiments reported in the paper (e.g., preliminary or failed experiments that didn't make it into the paper).

9. Code of ethics

Question: Does the research conducted in the paper conform, in every respect, with the NeurIPS Code of Ethics <https://neurips.cc/public/EthicsGuidelines>?

Answer: [Yes]

Justification: We confirm that our work complies with the NeurIPS Code of Ethics.

Guidelines:

- The answer NA means that the authors have not reviewed the NeurIPS Code of Ethics.
- If the authors answer No, they should explain the special circumstances that require a deviation from the Code of Ethics.
- The authors should make sure to preserve anonymity (e.g., if there is a special consideration due to laws or regulations in their jurisdiction).

10. Broader impacts

Question: Does the paper discuss both potential positive societal impacts and negative societal impacts of the work performed?

Answer: [NA]

Justification: We do not anticipate any specific negative societal impacts beyond those typically associated with standard machine learning research.

Guidelines:

- The answer NA means that there is no societal impact of the work performed.
- If the authors answer NA or No, they should explain why their work has no societal impact or why the paper does not address societal impact.
- Examples of negative societal impacts include potential malicious or unintended uses (e.g., disinformation, generating fake profiles, surveillance), fairness considerations (e.g., deployment of technologies that could make decisions that unfairly impact specific groups), privacy considerations, and security considerations.
- The conference expects that many papers will be foundational research and not tied to particular applications, let alone deployments. However, if there is a direct path to any negative applications, the authors should point it out. For example, it is legitimate to point out that an improvement in the quality of generative models could be used to generate deepfakes for disinformation. On the other hand, it is not needed to point out that a generic algorithm for optimizing neural networks could enable people to train models that generate Deepfakes faster.
- The authors should consider possible harms that could arise when the technology is being used as intended and functioning correctly, harms that could arise when the technology is being used as intended but gives incorrect results, and harms following from (intentional or unintentional) misuse of the technology.
- If there are negative societal impacts, the authors could also discuss possible mitigation strategies (e.g., gated release of models, providing defenses in addition to attacks, mechanisms for monitoring misuse, mechanisms to monitor how a system learns from feedback over time, improving the efficiency and accessibility of ML).

11. Safeguards

Question: Does the paper describe safeguards that have been put in place for responsible release of data or models that have a high risk for misuse (e.g., pretrained language models, image generators, or scraped datasets)?

Answer: [NA]

Justification: We did not identify any risks beyond those commonly associated with traditional machine learning research.

Guidelines:

- The answer NA means that the paper poses no such risks.
- Released models that have a high risk for misuse or dual-use should be released with necessary safeguards to allow for controlled use of the model, for example by requiring that users adhere to usage guidelines or restrictions to access the model or implementing safety filters.
- Datasets that have been scraped from the Internet could pose safety risks. The authors should describe how they avoided releasing unsafe images.
- We recognize that providing effective safeguards is challenging, and many papers do not require this, but we encourage authors to take this into account and make a best faith effort.

12. Licenses for existing assets

Question: Are the creators or original owners of assets (e.g., code, data, models), used in the paper, properly credited and are the license and terms of use explicitly mentioned and properly respected?

Answer: [Yes]

Justification: We provide dataset licenses, citation information, and detailed descriptions in Appendix A.14.1.

Guidelines:

- The answer NA means that the paper does not use existing assets.
- The authors should cite the original paper that produced the code package or dataset.
- The authors should state which version of the asset is used and, if possible, include a URL.
- The name of the license (e.g., CC-BY 4.0) should be included for each asset.
- For scraped data from a particular source (e.g., website), the copyright and terms of service of that source should be provided.
- If assets are released, the license, copyright information, and terms of use in the package should be provided. For popular datasets, paperswithcode.com/datasets has curated licenses for some datasets. Their licensing guide can help determine the license of a dataset.
- For existing datasets that are re-packaged, both the original license and the license of the derived asset (if it has changed) should be provided.
- If this information is not available online, the authors are encouraged to reach out to the asset's creators.

13. New assets

Question: Are new assets introduced in the paper well documented and is the documentation provided alongside the assets?

Answer: [NA]

Justification: [NA]

Guidelines:

- The answer NA means that the paper does not release new assets.
- Researchers should communicate the details of the dataset/code/model as part of their submissions via structured templates. This includes details about training, license, limitations, etc.
- The paper should discuss whether and how consent was obtained from people whose asset is used.
- At submission time, remember to anonymize your assets (if applicable). You can either create an anonymized URL or include an anonymized zip file.

14. Crowdsourcing and research with human subjects

Question: For crowdsourcing experiments and research with human subjects, does the paper include the full text of instructions given to participants and screenshots, if applicable, as well as details about compensation (if any)?

Answer: [NA]

Justification: [NA]

Guidelines:

- The answer NA means that the paper does not involve crowdsourcing nor research with human subjects.
- Including this information in the supplemental material is fine, but if the main contribution of the paper involves human subjects, then as much detail as possible should be included in the main paper.
- According to the NeurIPS Code of Ethics, workers involved in data collection, curation, or other labor should be paid at least the minimum wage in the country of the data collector.

15. Institutional review board (IRB) approvals or equivalent for research with human subjects

Question: Does the paper describe potential risks incurred by study participants, whether such risks were disclosed to the subjects, and whether Institutional Review Board (IRB) approvals (or an equivalent approval/review based on the requirements of your country or institution) were obtained?

Answer: [NA]

Justification: [NA]

Guidelines:

- The answer NA means that the paper does not involve crowdsourcing nor research with human subjects.
- Depending on the country in which research is conducted, IRB approval (or equivalent) may be required for any human subjects research. If you obtained IRB approval, you should clearly state this in the paper.
- We recognize that the procedures for this may vary significantly between institutions and locations, and we expect authors to adhere to the NeurIPS Code of Ethics and the guidelines for their institution.
- For initial submissions, do not include any information that would break anonymity (if applicable), such as the institution conducting the review.

16. **Declaration of LLM usage**

Question: Does the paper describe the usage of LLMs if it is an important, original, or non-standard component of the core methods in this research? Note that if the LLM is used only for writing, editing, or formatting purposes and does not impact the core methodology, scientific rigor, or originality of the research, declaration is not required.

Answer: [No]

Justification: We did not use LLMs for important, original, or non-standard component of the core methods.

Guidelines:

- The answer NA means that the core method development in this research does not involve LLMs as any important, original, or non-standard components.
- Please refer to our LLM policy (<https://neurips.cc/Conferences/2025/LLM>) for what should or should not be described.